Clean Technologies and Environmental Policy (2024) 26:1335–1362
https://doi.org/10.1007/s10098-023-02491-6

REVIEW

Exergy analysis of thermal desalination processes: a review

Z. Rahimi-Ahar[1] · M. S. Hatamipour[1]

Received: 22 August 2022 / Accepted: 16 February 2023 / Published online: 3 March 2023

Abstract

This study reviews the efforts made regarding thermal desalination systems, focusing on the exergetic aspect. Each plant has a component, which limits the magnitude of thermal energy improvement; however, the target should be an effort to minimize the exergy destruction. It was found that all stand-alone systems required modification or integration with other desalination plants due to their low exergy efficiency. Furthermore, the exergy-destructive components in humidification–dehumidification (HDH) systems as a domestic desalination process, in poly-generation systems by the ability of freshwater production and energy generation, and in combined cooling–heating–power (e.g., MEE-CCPP) cycles as the recent desalination technologies were introduced. The exergy efficiency of a desalination plant increased by coupling to a solid oxide fuel cell or heat pump, using surplus low-pressure or makeup steam and optimization of the effect and stage numbers. Designing a poly-generation system capable of producing power, desalinated water, as well as liquefied natural gas heating/cooling could improve the system exergetically. Desalination systems were found to benefit from increasing the evaporation temperature caused by a Rankine cycle. Coupling the HDH system to a reverse osmosis unit or thermo-compressor vapor compression–reverse osmosis plant was found to improve the system performance exergetically.

Graphical abstract

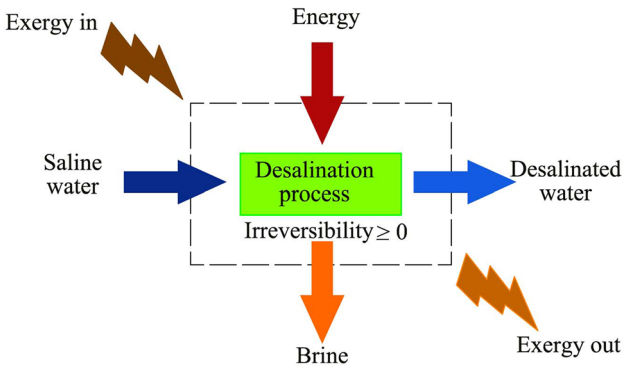

Keywords Thermodynamics · Thermal desalination · Exergy · Efficiency

Abbreviations

ACHP	Absorption–compression heat pump
AD	Adsorption desalination
BF	Backward feed
BR	Brine recirculation
CACW	Close air/close water
CAOW	Close air/open water
CCHP	Combined cooling–heating–power
EvGT	Evaporative gas turbine
FF	Forward feed
FFH	Forward feed with heater
GOR	Gained output ratio
GT	Gas turbine
GTC	Gas turbine cycle
HDH	Humidification–dehumidification

✉ M. S. Hatamipour
hatami@eng.ui.ac.ir

Z. Rahimi-Ahar
zohrehrahimi@eng.ui.ac.ir

[1] Chemical Engineering Department, University of Isfahan, Isfahan, Iran

HP	Heat pump
HRSG	Heat recovery steam generator
M	Mixer
MD	Membrane distillation
ME	Multi-effect
MEE	Multi-effect evaporation
MS	Multistage
MSF	Multistage flash
MVC	Mechanical vapor compression
OACW	Open-air/close water
OAOW	Open-air/open water
ORC	Organic Rankine cycle
OT	Once through
PF	Parallel flow
P/CF	Parallel/cross-feed
PRO	Pressure-retarded osmosis
PSA	Plataforma solar de almeriía
RC	Rankine cycle
RED	Reverse electrodialysis
RO	Reverse osmosis
SHC	Specific heat consumption
SOFC	Solid oxide fuel cell
SEC	Specific energy consumption
STIG	Steam-injected gas turbine
TBT	Top brine temperature
TVC	Thermo-compressor vapor compression
VC	Vapor compression
VCHP	Vapor compression heat pump
VHDH	Vacuum humidification–dehumidification
WGC	Waste gas chimney
ZEDS	Zero-emission desalination system
ZLD	Zero liquid discharge

List of symbols

b	Enthalpy coefficient
c	Entropy coefficient
Ex	Exergy (J)
ex	Specific exergy (J/kg)
G	Gibbs free energy (J)
$G^{'}$	Specific Gibbs free energy (J/kg)
g	Gravity (m/s^2)
I	Irreversibility (J)
$\dot{m}$	Mass flow rate (kg/s)
P	Pressure (Pa)
Q	Heat (J)
$\dot{Q}$	Heat transfer rate (W)
R	Gas constant (J/molK)
S	Entropy (J/K)
C	Specific heat (J/kgK)
s	Specific entropy (J/kgK)
T	Temperature (K)
U	Internal energy (J)
u	Specific internal energy (J/kg)
V	Velocity (m/s)
v	Specific volume (m^3/kg)
$\dot{W}$	Work transfer rate (W)
w	Salinity (kg/kg)
xX	Fraction of species
z	Altitude of the stream above the sea level (m)

Greek symbols

Δ	Difference
η	Efficiency
μ	Chemical potential (J/kg)

Subscript

0	Reference or ambient state
00	Dead state
e	Energy
gen	Generation
i	Counter
in	Incoming flow
out	Outcoming energy/exergy/stream flow
r	Room or ambient condition
s	Salinity
sw	Saline water

Introduction

Energy and water mainly affect the environment, social health and progress plans. Although many countries suffer from drinkable water scarcity, they mostly benefit from renewable or fossil fuel energy sources. Therefore, energy-efficient desalination technologies and devices should be developed to overcome the water shortage while meeting energy-saving requirements (Vadalia et al. 2014). During a process, the energy form simultaneously changes in quantity and quality (Ranjan and Kaushik 2013). Thermodynamic analysis of energy-consuming plants is a well-established tool for energy conservation in terms of quality and quantity.

Several desalination technologies have significantly developed in recent years and are expected to develop in the coming years from energetic, exergetic and economic viewpoints. Thermal desalination technologies involving phase change process include multistage flash (MSF), vapor compression (VC), multi-effect evaporation (MEE) and humidification–dehumidification (HDH) desalination processes (Li et al. 2013).

The energy efficiency of desalination plants is rated based on metrics such as specific energy or heat consumption (SEC/SHC), gained output ratio (GOR), second law efficiency and exergy efficiency (Altmann et al. 2019). The minimum work requirement for each distillation process depends on the properties of the outlet and inlet streams. An actual distillation process requires

a greater work input because of irreversibility (Cerci 2002). The minimization of exergy destruction is necessary to determine the operating conditions with optimum performance.

In this paper, the exergetic studies have been started through stand-alone thermal desalination plants (MSF (Slesarenko and Shtim, 1987), MEE (Guo et al. 2021), HDH (Alkhulaifi et al. 2021), VC (Farahat et al. 2021)) and continued with an investigation of integrated systems (MEE-VC (Rostamzadeh 2021), MEE-TVC-reverse osmosis unit (Shakib et al. 2021), desalination unit coupled to a heat pump (Lawal et al. 2018), and the exergy efficiency and exergy-destructive components were introduced. The exergy-destructive components in HDH system as a domestic desalination process, in poly-generation systems by the ability of freshwater production and energy generation, and in combined cooling–heating–power (e.g., MEE-CCPP) cycles as the recent desalination technologies are also presented for the first time in this paper (Kerme et al. 2020). In other published reviews, stand-alone desalination systems are reviewed exergetically (Gude 2018; Jamil et al. 2020). All proposed strategies are for energy recovery as well as the exergy efficiency optimization of the hybrid system. Heat recovery from hot distillate (Abid et al. 2021), using waste heat from industrial plants (Rafat and Babaelahi 2020) and using renewable energy sources (Omidi et al. 2020) are highly recommended in researches.

Methodology

Thermodynamic analysis is a well-known method for the characterization and energy/exergy optimization of a system. Desalination systems can be compared in terms of SEC which is defined by the ratio of desalination rate to input electrical energy. It is clear that the system performance improves when producing more freshwater while using less electrical energy. Exergy analysis evaluates how efficiently energy is used in a plant. Energy sources (regardless of being renewable or not) should be utilized through effective equipment during their end-use. To achieve energetic performance enhancement, a comprehensive understanding of the components' performance and overall system performance (freshwater productivity and energy consumption), an exergy-based approach is proposed to be used for a desalination process (Rahimi-Ahar et al. 2018). It means that exergy efficiency reveals more useful information than specific energy consumption. Many studies focused on such analysis for desalination processes, which are discussed in the next sections.

Exergy has the characteristic that it is conserved only when all processes of the system and the environment are reversible. The irreversibility in any real process leads to exergy consumption or destruction. The exergy consumption during a process is proportional to the entropy created due to the irreversibility associated with the process. When an exergy analysis is conducted on a desalination plant, the thermodynamic imperfections can be quantified as exergy destruction, which is wasted work or wasted potential for the production of work. Similar to energy, exergy can be transported or transferred across the boundary of a system (Dincer and Cengel 2001). The exergy technique associates each parameter with its exergy components: chemical, physical, kinetic and potential.

The quality of energy is measured by exergy which is inevitably destroyed in a real process. The second law states that a part of the exergy entering any thermal system by electricity, fuel or flowing streams of the matter is destroyed (energy degradation) within the system due to irreversibility. Therefore, the exergy flow into the system is always greater than that out of the system. The rate of exergy destruction (i.e., the difference between the inlet and outlet exergy contents) is called irreversibility (Dincer and Rosen 2012). The exergy balance of a system at steady state, in a control volume with inlet and outlet streams, due to the mass, energy, shaft work and electricity transfer, is described in Eq. 1 (Shukuya and Hammache 2002). The irreversibility rate is calculated via the Gouy–Stodola relation using the product of the entropy generation rate for all systems participating in the process and the temperature of the environment (see Eq. 2) (Kotas 1995).

Equations 3 and 4 calculate the exergy contents due to the stream flowing into and out of the system, respectively. The flow of exergy associated with heat transfer ($\dot{Q}$) is denoted by $\dot{Ex}_{heat}$ and can be expressed as Eq. 5 (Mastani Joybari et al. 2013). The exergy transfer associated with heat transfer depends on the temperature level at which it occurs in relation to the temperature of the environment. The total exergy can be broken into chemical, physical, kinetical and potential components (see Eq. 6). The physical and chemical exergies have been separated to enable the calculation of exergy values using standard chemical exergy tables. The potential and kinetic energies related to a stream of substance are fully convertible to work; hence, they are equal to potential and kinetic exergies, respectively (Eqs. 7, 8). Mostly the exergy analysis of a seawater desalination unit can be modeled by considering a mixture of solid sodium chloride and liquid water (Sharqawy et al. 2011).

$$\dot{Ex}_{in} + \dot{Ex}_{heat} = \dot{Ex}_{out} + \dot{Ex}_{work} + I \quad (1)$$

$$I = T_0 \dot{S}_{\text{gen}} = T_0 \left(\sum \dot{m}_{\text{out}} s_{\text{out}} - \sum \dot{m}_{\text{in}} s_{\text{in}} - \sum_r \frac{\dot{Q}_r}{T_r} \right) \quad (2)$$

$$\dot{E}x_{\text{in}} = \sum \dot{m}_{\text{in}} ex_{\text{in}} \quad (3)$$

$$\dot{E}x_{\text{out}} = \sum \dot{m}_{\text{out}} ex_{\text{out}} \quad (4)$$

$$\dot{E}x_{\text{heat}} = \sum_r \dot{Q}_r \left(1 - \frac{T_0}{T_r}\right)_{\text{in}} - \sum_r \dot{Q}_r \left(1 - \frac{T_0}{T_r}\right)_{\text{out}} \quad (5)$$

$$ex = ex_{physical} + ex_{chemical} + ex_{kinetic} + ex_{potential} \quad (6)$$

$$ex_{\text{potential}} = g(z - z_0) \quad (7)$$

$$ex_{\text{kinetic}} = \frac{V^2 - V_0^2}{2} \quad (8)$$

The exergy of a substance consists of a physical part and a chemical part. The latter is attributed to the chemical formation of the substance in the standard state from the exergy reference level substance in the environment. On the other hand, the physical part of exergy is attributed to the changes in temperature, pressure and concentration (mixing) of the substances. Physical exergy (Eq. 9) is equivalent to the maximum work obtained when flow rate or pressure and temperature of the system moves from a certain thermodynamic state to the reference state (denoted by the subscript 0) with no change in concentration.

$$ex_{\text{physical}} = u - u_0 + P_0(v - v_0) - T_0(s - s_0) \quad (9)$$

For a perfect gas and solid/liquid (compressible substance assumption) mixture, the physical exergy is calculated by Eqs. (10) and (11), respectively (Tiwari and Sahota 2018):

$$ex_{\text{physical}} = C[(T - T_0) - T_0 ln \frac{T}{T_0}] + RT_0 ln \frac{P}{P_0} \quad (10)$$

$$ex_{\text{physical}} = C[(T - T_0) - T_0 ln \frac{T}{T_0}] + v(P - P_0) \quad (11)$$

Any chemical substance has a chemical energy content in terms of its chemical potential along with its chemical exergy (Sato 2004). The chemical exergy determines the maximum work achieved when the concentration of each substance in the system is taken from the reference state (denoted by the subscript 00) up to the dead state. Chemical exergy is calculated in the processes involving heat transfer and exchange of substances only with the environment (Kotas 1995). The chemical exergy is formulated as:

$$ex_{\text{chemical}} = \sum_{i=1}^{n} \mu_{00,i} w_s = (\mu_i - \mu_{00,i}) w_s \quad (12)$$

where μ_i and $\mu_{00,i}$ are the chemical potentials of component i at (T_{00}, P_{00}, w_s) and (T_{00}, P_{00}, w_{s00}), respectively (Al-Weshahi et al. 2013). The chemical part becomes in terms of mole fraction as:

$$ex_{\text{chemical}} = RT_0 \sum X_i ln(X_i / X_{i0}) \quad (13)$$

The chemical potential of seawater is calculated by differentiating the Gibbs function as:

$$\mu_s = \frac{\partial G_{sw}}{\partial m_s} = g_{sw} + (1 - w_s) \frac{\partial G'_{sw}}{\partial w_s} \quad (14)$$

$$G'_{sw} = h_{sw} - (T + 273.15) s_{sw} \quad (15)$$

$$h_{sw} = b_1 w_s + b_2 w_s^2 + b_3 w_s^3 + b_4 w_s^4 + (b_5 T + b_6 T^2 + b_7 T^3) w_s + b_8 w_s^2 T + b_9 w_s^3 T + b_{10} w_s^2 T^2 \quad (16)$$

$$s_{sw} = c_1 w_s + c_2 w_s^2 + c_3 w_s^3 + c_4 w_s^4 + (c_5 T + c_6 T^2 + c_7 T^3) w_s + c_8 w_s^2 T + c_9 w_s^3 T + c_{10} w_s^2 T^2 \quad (17)$$

In the literature, several expressions have been defined to quantify the exergy performance of a process, two of which are presented here. An efficiency based on total exergy accounts for thermodynamic losses (referred to as irreversibility) in the processes, such as the ones caused by heat transfer, chemical reaction, mixing and unrestricted expansion. The first definition (Eq. 18) called the degree of perfection was introduced by Szargut et al. (1988):

$$\varepsilon = \frac{\dot{E}x_{\text{useful.products}}}{\dot{E}x_{\text{feeding}}} \quad (18)$$

The second expression is used in the analysis of thermal processes as:

$$\varepsilon = \frac{\dot{E}x_{\text{Useful}}}{\dot{E}x_{\text{Driving}}} \quad (19)$$

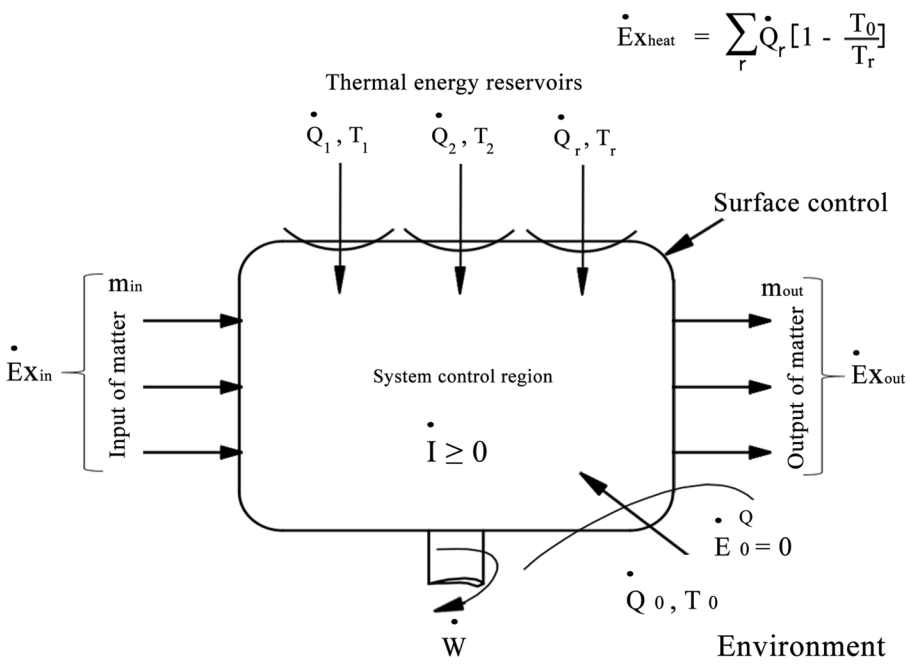

Fig. 1 An exergetic view of a desalination plant (Spiegler and El-Sayed 2001)

Thermodynamic analysis of different thermal desalination units based on energy as well as exergy can be categorized as:

- MSF, MEE, VC and HDH systems are studied exergetically.
- These thermal desalination processes are hybridized with each other or other non-thermal desalination technologies such as reverse osmosis (RO) or membrane distillation (MD).
- The heat pump (HP) or Rankine cycle (RC) also can be coupled to desalination plants to increase productivity and improve their exergetic performance.

Process optimization is achieved by finding the optimal operating conditions and modifying the components, hence decreasing the exergy destruction.

For desalination plants, Spiegler and El-Sayed (2001) proposed an approach to allocating the minimum work of separation as the exergy of the produced brine and freshwater. This approach is presented in Fig. 1 (Spiegler and El-Sayed 2001).

Consider a simple black-box separator model for a desalination system. The required work for separation entering the system is denoted by $\dot{W}$, and the heat transfer into the system is $\dot{Q}$. Stream feedwater is the incoming seawater; stream desalinated is a product, while another outlet stream is the concentrated reject brine. Product and reject streams may exit the desalination system at temperatures different from the ambient conditions. The exergy associated with these streams could be used to produce some work that would offset the required work of separation. However, if the exergy associated with thermal disequilibrium is not harnessed in this way, but simply discarded, entropy is generated as the streams are brought to the thermal equilibrium with the environment. Similarly, pressure disequilibrium results in additional entropy generation. Differences in concentration between various streams represent a chemical disequilibrium that could be used to produce additional work. However, since the purpose of the desalination plant is to split a single stream into two streams of different concentrations, the outlet streams are not brought to chemical equilibrium with the environment. The inlet exergies are the exergy content of the inlet saline water (via its mass flow rate, physical and chemical exergy contents) and the heat exergy (generated by electrical or renewable energy sources) while the outlet exergies are the exergy consumed by the pump(s) and compressor(s) and the exergy content of the produced freshwater and concentrated brine (Zhou et al. 2020). The exergy transfer associated with work is equal to the work. The exergy efficiency of the desalination plant is defined using Eq. 20 (Shukuya and Hammache 2002).

$$\eta = \frac{\sum \dot{E}x_{\text{exit}}}{\sum \dot{E}x_{\text{inlet}}} = \frac{\dot{E}x_{\text{Power}_{\text{output}}} + \dot{E}x_{\text{Freshwater}} + \dot{E}x_{\text{Brine}} + (\dot{E}x_{\text{heat}})_{\text{out}}}{\sum(\dot{E}x_{\text{chemical}} + \dot{E}x_{\text{physical}})_{\text{Feedstream}} + (\dot{E}x_{heat})_{\text{in}}} \quad (20)$$

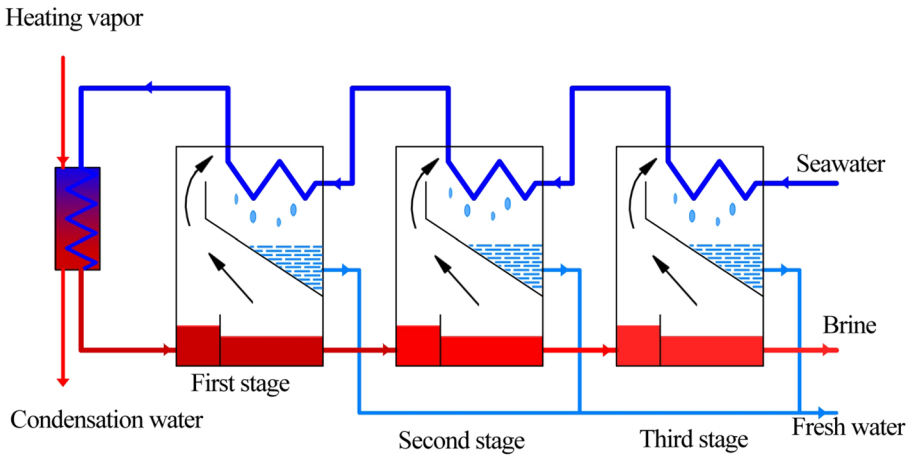

Fig. 2 Schematic representation of an MSF desalination system (Woldai 2016)

Exergy analysis of thermal desalination processes

Simultaneous energy, exergy and exergoeconomic studies provide a thorough analysis to have a profound understanding of the energy consumption, irreversibility and cost related to the irreversibility of each cycle, leading to process optimization.

Multistage flash desalination

The MSF desalination plants supply freshwater to many areas. Figure 2 shows the schematic diagram of an MSF desalination system. According to the figure, the seawater is heated by steam in the first stage which then flows into a series of stages. The pressure decreases in the succeeding stages, and the driving force for evaporation rises through differential pressure between the stages. The unevaporated seawater in the first stage moves into the second stage and this procedure continues until the last stage. The released vapor generates the desalinated water, while its condensation enthalpy is simultaneously transferred to the entering seawater (Rahimi-Ahar et al. 2020a).

An MSF plant includes brine heating followed by flash distillation in several stages to recover the heat. Once through (OT), simple mixer (M) and brine recirculation (BR) designs have been proposed (Mussati et al 2004). In the MSF-OT design, the total brine passes once through the process, while in the MSF-M design, part of the concentrated brine is mixed with the incoming feedwater. In the MSF-BR design, the seawater mixes with the brine leaving the last stage. Among the three proposed designs, the MSF-OT is the simplest one, while the MSF-BR is the most efficient design (Bandi et al. 2016). The performance is improved by recovering the released heat from the distillate in the MSF stages and increasing the temperature of makeup seawater (Al-weshahi et al. 2014). Most of the exergy exiting the early stages is destroyed in the vacuum system by subsequent mixing with stages at lower temperatures. Hence, distillate water recovery from the early stages and utilizing its exergy for another process such as MEE, district heating or organic Rankine cycle (ORC) could improve the second law efficiency of the MSF process (Ghaffour et al. 2015). The high feed temperature in the summer reduces the evaporation rate of any MSF plant and hence its freshwater productivity (Alhazmy 2014). To address this, a cooler and a mixing chamber at the feed path could be installed; however, this could increase the freshwater production cost.

Exergy analysis of an MSF system (capacity of 3800 m^3/h) was conducted using IPSEpro software (Al-Weshahi et al. 2013). The exergy inlet to the unit was the summation of the pump work and heating steam, while the output minimum separation work was the sum of the distillate and drained brine relative to the exergy of the cooling water. The overall exergy efficiency of 5.8% was reported. From 64% of the destructed exergy in the evaporator, 54% and 10% were related to the heat recovery in stages 1 to 16 and the heat rejection in stages 17–19, respectively. Moreover, 4%, 17% and 13% of exergy destructions were associated with the brine heater, pumps and stream disposal, respectively. Furthermore, the study confirmed that the lowest exergy destruction occurred in the first stage, augmented gradually in the heat recovery stages and sharply in the heat rejection stages, showing that exergy destruction increases from the high-temperature stages to the low-temperature ones. Through the heat recovery from the distillate, the unit exergy efficiency increased up to an almost acceptable value of 14%.

Different MSF units (capacity of 11,365–34,095 m^3/d) designed by Saline Water Conversion Corporation were characterized exergetically by Hamed et al. (2000). The number of stages varied between 16 and 34, while the operating top brine temperature (TBT) varied in the range of 90–115 °C. The specific exergy destructions were dependent

upon the specific condensing area, TBT and number of stages. The system which operated at a high TBT and high flash stage number had low exergy destruction. Conversely, in the system with high TBT and low condensing area, the exergy destruction was high. For all studied systems, the majority of exergy destruction occurred in the heat recovery section (more than half), followed by the heat rejection section, brine heater and leaving streams.

The exergy destruction in an MSF plant located in Yanbu, Saudi Arabia, was determined through a non-iterative code in MATLAB by Al Ghamdi and Mustafa (2016). The major exergy destruction of ~ 75% occurred in the heat recovery section. By increasing the stage number from 25 to 31, the exergy destruction decreased from 75 to 69%. It means that it was reasonable to operate the system for more than 25 stages in the peak load. The exergy destruction values in the heat rejection section with 3 and 25 stages were 20% and 75%, respectively. Hence, removing the heat rejection section and increasing the number of stages in the heat recovery section were recommended. The overall second law efficiencies of 2.8% and 3.2% were calculated at peak and normal loads, respectively. The second law efficiency could be improved by reducing the inlet exergy to the system and controlling the exergy destructions during operation. To improve the system performance exergetically, recycling brine into the mixing tank instead of the last stage of the heat recovery section, eliminating the flow and temperature control of seawater intake, coupling the preheater tubes to the heat recovery section for continuous feedwater flow and using a low capacity pump for intake seawater were recommended. It was concluded that the MSF-M design was a practical option to lower the exergy destruction compared to the MSF-OT design. Removing the heat recovery section and increasing the number of stages by either converting it to MSF-BR or MSF-M design can be the best idea for MSF design.

Exergy analysis of an MSF process using the developed visual design and package was carried out by Nafey et al. (2006a). Using this developed package, an exergy efficiency of 1.87% was obtained. The results indicated that the desuperheater and pumps had low exergy efficiency while the highest irreversibility occurred in the flash chambers. The exergy input to the system was decreased by load reduction due to a decrease in steam consumption and pumping power. Reducing the MSF capacity lowered the exergy of the distillate due to the decrease in the product flow rate. The decrease in exergy efficiency with the capacity reduction indicated that the exergy output was dominant. It means an MSF system benefited from increasing the system capacity while decreasing the exergy input; this aim can be obtained by increasing the flash stage number.

Exergy destructions in three MSF plants with 16, 19 and 22 stages and capacities of 194,170 m^3/d, 181,818 m^3/d and 940,000 m^3/d, respectively, conducted by Al-Sulaiman and Ismail (1995). The results revealed that the proposed MSF plants were highly exergy-destructive with exergy efficiencies in the range of 1.12–10.38%. The brine heaters consumed about 13–29% of the total exergy. It was concluded that the TBT was proportional to the exergy destruction in all plants. The exergy contents were very sensitive to temperature variation and water salinity. A smaller temperature difference between the flashing chambers decreased the exergy destruction. A reduction in temperature difference was achieved by increasing the size of the last stages to compensate for the reduction in vapor density (increase in its velocity) to increase the entrainment of brine droplets. It means that for a given finite temperature difference, using more stages and increasing the size of the last stages resulted in a higher exergy efficiency.

An exergy analysis on an MSF (0.871×10^6 m^3/d) unit was conducted by actual operation data (Kahraman and Cengel 2005). The highest exergy destruction of ~ 78% occurred within the MSF, indicating that the flashing process itself was highly inefficient. The exergy destruction was decreased by increasing the number of flashing stages. Among the components, the performance of motors and pumps with an exergy destruction contribution of 5.3% could be improved

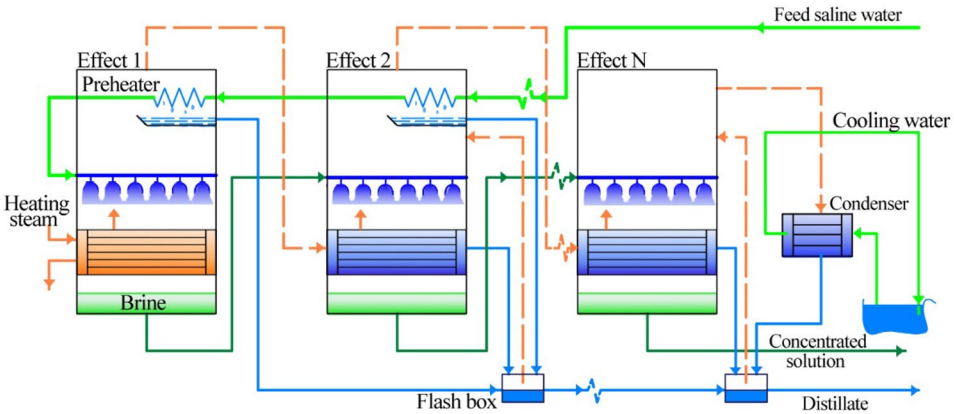

Fig. 3 Schematic representation of an MEE desalination system (Rahimi and Chua 2017)

using more efficient types. A low second law efficiency of 4.2% confirmed that there were opportunities in the plant to lower the exergy destruction rate. Burning fuel imposed a high amount of additional exergy destruction. Exergy efficiency enhancement could be achieved by designing cogeneration with an electricity generating plant, using high-temperature steam and using the heat exchanger of the MSF plant as a condenser.

Multi-effect evaporation

Generally, MEE is used for medium-scale to large-scale (less than 0.015×10^6 up to 0.025×10^6 m^3/d) desalinate water production plants. Such plants are comprised of a series of evaporators in which evaporation occurs due to recovering the enthalpy of phase change. The generated vapor in the first effect (evaporator) moves to the second effect to evaporate part of the saline water leaving the first effect. The produced vapor flows to the third effect due to the lower pressure compared to the previous effects. This process continues to the last effect, where the vapor flows to the condenser (Messineo and Marchese 2008). The enthalpy of phase change of the produced vapors in the previous effects is used for the next effect (Ghaffour et al. 2015). There are different feeding configurations of MEE plants such as backward feed (MEE-BF), parallel flow (MEE-PF), parallel/cross-feed (MEE-P/CF), forward feed (MEE-FF) and forward feed with heater (MEE-FFH). Among them, MEE-FFH and MEE-PF were found to be more efficient (Elsayed et al. 2018a). The schematic of an MEE system is presented in Fig. 3.

The work potential of the recovered energy in an MEE plant operating at low pressure was studied by Sundari et al. (2013). Exergetic analysis was performed at evaporator pressures in the range of 1.3–2.3 kPa. It was proved that the flow exergy of a control volume might have a negative or positive value depending on the evaporator pressure. Once the pressure and temperature were equal to the dead state, the exergy was positive. When the temperature was higher or lower than this dead state, the exergy was also positive. The flow stream could be expanded via a turbine and could produce work resulting in positive flow exergy ($P > P_0$). This work could be utilized to compress the flow stream via a compressor causing negative flow exergy ($P < P_0$). The highest exergy destruction occurred in the evaporator followed by the condenser. This system with an exergy efficiency of ~ 3% was comparable with the MSF and HDH processes with exergy efficiencies of 4% and 5.7%, respectively.

Thermodynamic analysis of an MEE system integrated into a utility steam network demonstrated that utilizing steam from a medium-pressure source resulted in the maximum freshwater production rate while using steam from a low-pressure source caused the highest exergy efficiency. In three-effect and eight-effect MEE units, changing the compression ratio from 2 to 5 decreased the exergy efficiency by 50% and 54%, respectively. It means that an MEE system with more effects was sensitive to the compression ratio and higher pressure eased the energy recovery; hence, freshwater productivity was enhanced. In addition, increasing the effect number reduced the temperature difference between the effects as well as between each effect and heat exchanger, lowering the exergy destruction. Increasing the pressure ratio from the first to the last effect resulted in a higher-temperature difference between the effects, increasing the exergy destruction (Salimi et al. 2018).

An MEE process was optimized via a thermo-economic-aided technique using pinch-based plant retrofit by Piacentino and Cardona (2010). The process was optimized through a creative structure for the effects, reflecting the interactions among exergy flows. While the temperature difference between two consecutive effects increased, the preheaters and the heat exchanges became the main sources of irreversibility. Neglecting flashing at brine inlet, cascade heating and limiting exergy destruction at the preheaters were proposed for process optimization. Auxiliary systems such as a heater can be used whenever the temperature difference between two consecutive effects increases. Moreover, a higher heat source temperature should be used to greatly improve spray evaporation and reduce the size of the evaporator.

El-Nashar and Al-Baghdadi developed an MEE system based on exergy destruction (El-Nashar and Al-Baghdadi 1998). Based on measured data, the discharge streams of distillate, brine and seawater accounted for the highest destruction (34.9% of the total), followed by the vacuum pump (30% of the total). Exergy destruction due to pressure drop and heat transfer in the preheaters, last condenser, brine flashing chamber and distillate between the successive effects accounted for the significant exergy destruction contribution in the evaporator (10.8%). The first effect was responsible for a large amount of irreversibility due to the high heat transfer, but it was reduced when using steam as the heating agent.

Khalilzadeh and Hossein Nezhad designed an MEE system using the waste heat released by a wind turbine (Khalilzadeh and Nezhad 2018). The highest exergy destruction was associated with the second effect. Recycling the waste heat increased the exergy efficiency by 7.34%. The MEE unit and overall exergy efficiencies were 10.92% and 0.085%, respectively. The first preheater of the desalination unit and the first effect had the lowest and highest exergy efficiencies, respectively.

A parametric study of an MEE system was conducted at CIEMAT-Plataforma Solar de Almería (PSA) (Carballo et al. 2018). It was found that the main source of exergy consumption was different from the main source of energy consumption. The outlet water stream from the evaporator

was used by the heat source in the PSA facility. This stream returned to the inlet water stream into the evaporator. Therefore, it did not represent a significant energy consumption while the maximum exergy destruction occurred in the evaporator.

The heat released from the liquid fuel production process of natural gas was applied using Fischer–Tropsch synthesis for a cogeneration process (Shariati et al. 2019). The integrated structure had an overall exergy efficiency of 79.53%. The maximum exergy destruction ratio of 31.4% occurred in the reforming reactors. The heat exchanger and expansion valve achieved exergy efficiency values of about 98.5% and 49.1%, respectively. The lowest exergy efficiency of 1.86% occurred in the MEE system. Integration of spray evaporation and MEE achieved zero liquid discharge (ZLD). The highest exergy destruction about 68% occurred in the evaporation tank. The useful exergy efficiency was 1.13%, and a large amount of excess exergy was wasted in the process of achieving ZLD (Guo et al. 2021). Notably, different from the conventional MEE systems, the spray evaporation-MEE system achieved better performance with fewer effects due to the highest exergy destruction in the spray evaporator.

Vapor compression

In the VC process, the saline water boils whose generated vapor condenses via compression, producing the desalinated water. Unlike the MSF and MEE processes, where the thermal energy of the brine is degraded, it is upgraded to evaporate more brine in the VC process. VC units are comprised of a mechanical vapor compressor or thermo-compressor,

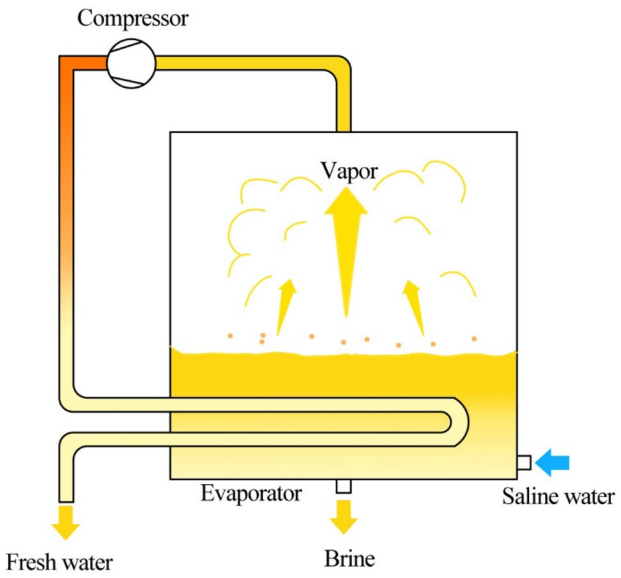

Fig. 4 Schematic representation of a VC desalination system (Senatore 1979)

evaporator, condenser, preheaters, brine and product pumps (Messineo and Marchese 2008). The VC suffers from scale formation in the boiler. Moreover, it is not appropriate for places with large-scale low-grade energy. Therefore, combining VC with MSF or MEE systems contributes to more energy utilization (Zheng 2017). The schematic representation of a VC desalination system is presented in Fig. 4.

The main role of ejector performance on exergy efficiency in VC desalination systems shows why the ejector design improvement has been ongoing (Tang et al. 2018).

Jamil and Zubair (2017) presented an exergy-based analysis of each component used in a forward feed-mechanical vapor compression (FF-MVC) system to highlight the contribution of each component to the overall exergy destruction. The evaporators had ~ 95% exergy destruction accounting for the highest amount because of high operating temperature and phase change heat transfer. Their exergy destruction decreased as the stage number was increased owing to a reduction in the amount of distillate and heat load in each evaporator, therefore decreasing the temperature drop which in turn reduced the exergy destruction. The distillate, pumps and brine preheater had the maximum exergy destruction contribution values of 3.6%, 1% and 0.8%, respectively. An MVC plant with nano-filtration pretreatment was developed in which the required electrical and thermal energies were generated by the PV panel and parabolic trough collectors. The improvement in exergy efficiency was 153.7%, 56.3%, 32.6% and 27% compared with MEE-MVC and conventional VC, FF-ME-MVC and RO systems, respectively. The PV panel and solar collector had the highest shares in exergy destruction at 85.79% and 69.53%, respectively. The salt rejection and recovery ratio were the most important parameters to augment the exergy efficiency (Farahat et al. 2021). A VC flash desalination process was studied based on exergy analysis by Jin et al. (2014). They found that the exergy destruction by the flash tank was the highest followed by the heat exchanger, compressor and auxiliary electric heater. The exergetic performance of the process was improved by increasing the areas of the heaters and heat exchangers, increasing the flash tank volume and using a high-efficiency heat exchanger. Using a high-efficiency compressor with a low compression ratio was also recommended for process enhancement.

The performance of a four-effect thermo-compressor vapor compression (TVC) system was analyzed by Hamed et al. (1996). The TVC had the least exergy destruction rate among its counterparts, most of which occurred in the first effect and thermo-compressor. Increasing the entrainment ratio of the thermo-compressor and the number of effects, as well as reducing the TBT and heating steam temperature significantly increased the exergy efficiency. For all three investigated systems, the maximum exergy destruction was related to the first effect, due to the high temperature of the

consumed steam providing heat to the first effect. The mass and heat transfer in high exergy-destructive components should be studied in more detail to clarify the inner-mixing process and its effect on the entrainment ratio.

The performance of a TVC system was improved by integrating a spray-assisted desalination unit (Chen et al. 2019). The steam jet ejector was the main source of irreversibility, accounting for above 40% of the total exergy destruction. The process was enhanced at a higher number of stages, a lower motive steam pressure and a medium value of the cooling water flow rate. Other main sources of exergy destruction were the condensers, evaporators and heat exchangers. This result differed from that of a spray-assisted system, where the condenser was the major source of irreversibility. The integrated system had the minimum exergy destruction rate when the vapor was entrained from the third evaporator (due to its minimum irreversibility), leading to higher irreversibility in the VC and making the third stage the best location for vapor entrainment. The system became more exergy-destructive when the motive steam pressure was increased.

Various operating parameters of a freezing unit working on a reversed VC cycle were exergetically analyzed by Abd Elrahman et al. (2020). The results showed that recycling larger quantities of the discharged brine was more effective owing to the increase in the thermal efficiency of the operating cycle. A part of the brine should be recycled and mixed with the feedwater to reduce the exergy destruction. The compressor followed by the expansion valve, reversed condensers and evaporator had the highest second law efficiency. Chung et al. (2017) proposed a ZLD process containing an MVC for brine concentration and an MEE for crystallization. A salinity-gradient power production technology such as pressure-retarded osmosis (PRO) could be used due to its higher energy density. The second law efficiency of the evaporator increased by ~ 70% as the heating source temperature was reduced from 100 °C to 80 °C. The minimum required work in the proposed process was reduced by utilizing a low-grade energy source, decreasing the top temperature by an increase in the heat exchanger area, brine management using the generated power via a PRO and brine mixing with a feed with low salinity. A zero-emission desalination system (ZEDS), including a single-stage as well as a multistage (MS) MVC process, was introduced by Han et al. (2017). The results showed that the MS-ZEDS could decrease the compressor power consumption compared to the single-stage one. It was found that increasing the intermediary concentration at the outlet of the first stage minimized the exergy destruction.

Humidification–dehumidification

HDH is a small-scale thermal-based desalination technique in which humidification and dehumidification procedures are carried out in a humidifier and a condenser, respectively. The open-air/open water (OAOW), open-air/close water (OACW), close air/close water (CACW) and close air/open water (CAOW) configurations have been introduced. The closed cycles of air and water recover energy from the HDH system. However, for the closed water cycles, the scale formation and brine recirculation percentage should be considered. Water and air heating are the usual strategies for accelerating the evaporation rate (Yildirim and Solmuş, 2014). HDH system has better exergy efficiency in dry air environment compared to humid air environment (Aziz et al. 2022). The schematic representation of a water-heated HDH system is illustrated in Fig. 5.

The separation of water vapor from the air is an irreversible process, resulting in exergy destruction, which can be calculated. Increasing the inlet air temperature into the dehumidifier decreases the latent heat of vapor condensation, lowering the energy required to condense the unit mass of desalinated water. For the initial water temperature of 30 °C, about 12.7 kWh of energy per ton of desalinated

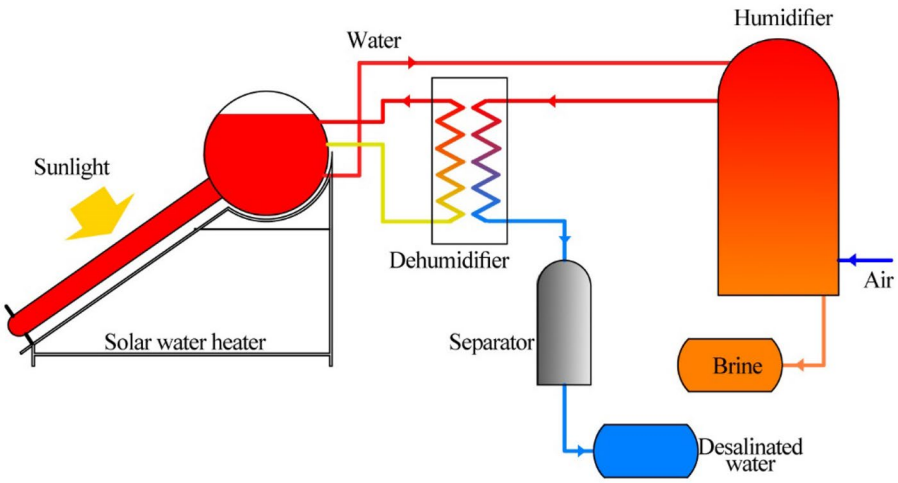

Fig. 5 Schematic representation of an HDH desalination system (Rahimi-Ahar et al. 2020a)

water is required, which is about 10 times higher than the minimum work required for the flash operation. It proves that the energy recovery process is essentially required for HDH systems to enhance their thermal efficiency (Zheng 2017). It can be deduced from the literature that the minimum amount of work required for seawater desalination should be estimated for various saline water concentrations (Zheng 2017). Notably, the evaporation work is almost linearly proportional to the salt mass concentration. Wu et al. (2017) proved that a higher feed salinity increases the minimum work.

Many scholars have thermodynamically analyzed some HDH plants which are summarized in this section. For instance, a solar-assisted HDH unit was exergetically studied by Elhaj and Yassin (2013). It was revealed that the humidifier exergy efficiency increased by increasing the air-to-water mass ratio and reducing the outlet air temperature. At low air temperatures, no noticeable impact on the humidifier exergy efficiency was concluded when changing the air-to-water mass ratio, while at air temperatures above 60 °C, the efficiency increased. Besides, the condenser exergy efficiency was increased with the increase in the outlet air temperature from the humidifier and the mass ratio. It was due to an increase in the energy loss to the environment. In a 2-stage HDH system with different cooling media (normal and chilled water), for a high water flow rate, an increase in air temperature increased the second law efficiency up to a certain value beyond which it started to decrease (Chiranjeevi and Srinivas 2016). A reverse trend was observed for a low water flow rate. In a waste-driven HDH process, similar results were concluded (He et al. 2016).

Ashrafizadeh et al. (2012) described a new technique for exergy analysis of HDH systems entitled the driving force approach using the sink–source concept. It was concluded that the mass transfer phenomenon did not have a significant influence on the exergy destructions of the air- and water-heated HDH systems while the flow rate of the unheated stream and the highest process temperature played the main roles in the overall exergy destruction. It was observed that ~ 90% of the overall loss was related to the heater and no exergy destruction occurred due to the mass transfer across the desalination processes. The heater followed by the dehumidifier and humidifier was the largest irreversibility sources. Higher air flow rates led to more heater load, increasing the exergy destruction. The large exergy destruction via the solar collector and rejected brine in the solar HDH process could be decreased by insulation, heater optimization and reusing the rejected water (Hou et al. 2007). Muthusamy and Srithar (2017) studied an HDH system to save the input power by modifying its components. The air heater was equipped with two types of inserts. The usage of inserts increased the outlet air temperature from the heater and humidifier, improving the humid air generation and exergy efficiency. The exergy efficiency of the air heater was gradually enhanced by decreasing the pitch ratio, increasing the orientation angle for the circular insert and using the divergent type for two other inserts. As the water heater followed by the humidifier, dehumidifier and air heater had the lowest highest exergy efficiency, they should be considered in the same order to enhance the system's exergetic performance.

An HDH system using solar energy to provide thermal, as well as electrical energy was proposed by Deniz and Çınar (2016). The highest exergy efficiency value of 1.87% was achieved. The maximum daily exergy and energy efficiencies were decreased near the sunset time because of using the energy stored earlier. Exergy destruction in the solar air and water heaters occurred through the glass covers as well as the bottom and sidewalls of the PV panel. The exergy destruction by heaters was contrariwise proportional to the ambient temperature while exergy destruction from the PV panel increased by increasing the ambient temperature. The most critical component of the proposed plant was the condenser where the humid air temperature was decreased to completely condense the moisture. The exergy of the PV panel reduced during the daytime because of the increase in its back-surface temperature, depending on the ambient condition.

A mathematical model of an air-heated HDH system was developed by Nematollahi et al. (2013). At a constant humidifier volume, the exergy efficiency could reach its maximum when a shorter humidifier with a larger diameter was designed. Increasing the humidifier diameter reduced the outlet air humidity as well as outlet air and brine temperatures from the humidifier due to the dependency of the mass and heat transfer coefficients on the humidifier diameter. The air exergy through convective heat transfer significantly increased from the top to the bottom of the humidifier in accordance with its temperature rise.

Exergy analysis was conducted on a variable pressure HDH system, indicating that the compressor and throttle valve improved the dehumidification and humidification processes, respectively (Sharqawy et al. 2017). It was found that increasing the dehumidifier-to-humidifier pressure ratio increased the exergy destruction, whereas the top feed temperature did not affect the irreversibility up to 60 °C. The pressure ratio of 1.33 and the humidifier and dehumidifier effectiveness values of 0.8 resulted in the lowest specific exergy destruction. Rahimi-Ahar et al. (2020b) exergetically analyzed a vacuum humidification–dehumidification (VHDH) system. The majority of irreversibility was found to be caused by the vacuum pump. In their previous study (Rahimi-Ahar et al. 2018), it was concluded that the VHDH system benefited from lower humidifier pressures from the freshwater productivity viewpoint, while in terms of exergy the pressure reduction increased the irreversibility. Simultaneous theoretical and experimental studies confirmed that

freshwater productivity, as well as energy and exergy efficiencies, could all be the deciding factors for the determination of desired values of parameters achieved, respectively.

An ultrasonic humidifier was used in an HDH system by Feng et al. (2018). It was concluded that higher relative humidity values decreased the exergy destruction. Increasing the relative humidity up to 60%, the exergy destructions of ultrasonic and steam systems were 0.28 kJ/kg and 0.34 kJ/kg, respectively. It was due to the high exergy content of the humid air at high relative humidity, leading to more irreversibility. The ultrasonic humidifier had superior performance to the steam system based on energy saving and exergy efficiency. The total irreversibility in the ultrasonic humidification (isenthalpic process) was lower than in the steam-based system (isothermal process). Using the fogging to nozzles in an HDH plant impacted the system performance positively in terms of improving the exergy efficiency due to higher condensation and evaporation rates and recovered energy (Alrbai et al. 2022). A lack of information was found in the exergy analysis of an HDH system containing a bubble column humidifier and dehumidifier. As bubble column-assisted HDH systems provide enhanced heat and mass transfer, their exergy analysis would reveal interesting results against ranking the exergy-destructive components.

Hybrid and cogeneration desalination systems

Three layouts of a hybrid thermal desalination system (capacity of 0.04 million m^3/d) containing waste gas chimney (WGC), gas turbine cycle (GTC) and ORC were

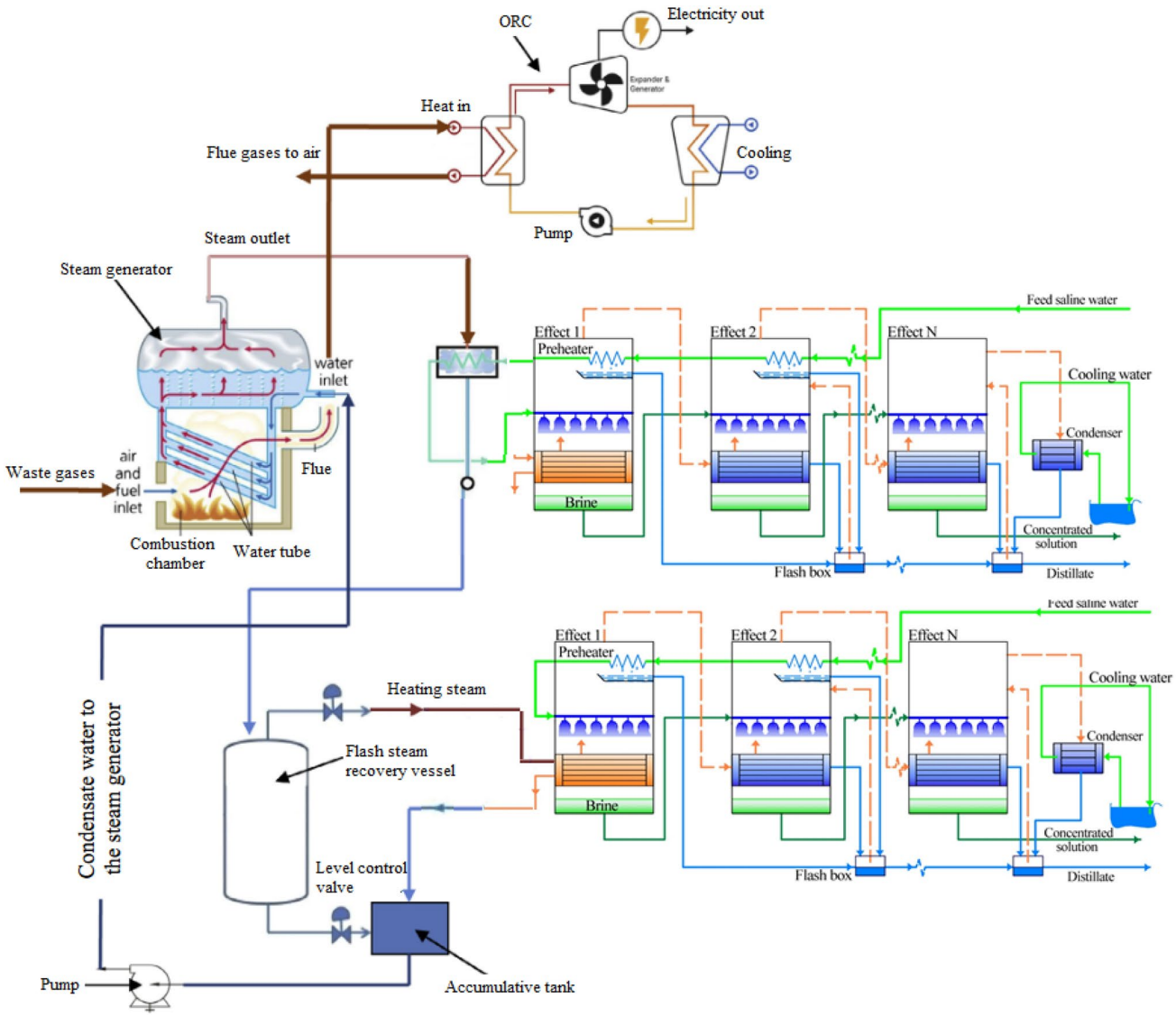

Fig. 6 A schematic of the WGC-MEE-GTC-ORC system

investigated by Sharaf and Soliman (2017). These layouts were designed as WGC-MSF-MEE, WGC-MSF-MEE-ORC and WGC-MSF-GTC. Using waste gases instead of natural gas saved 1136 $/h. The third layout had noteworthy results by achieving an exergy efficiency of 62.7% due to its high power generation. The generator, MEE, MSF and combustion chamber recorded substantial exergy destructions. WGC-MEE-GTC-ORC system can be arranged as shown in Fig. 6. By replacing the MSF unit instead of the MEE plant in the hybrid system, the freshwater productivity and exergy efficiency was improved.

An MSF–MVC process proposed by Alasfour and Abdulrahim showed that by increasing the temperature drop across the stages, the SEC and exergy destruction increased while the distillate water production decreased (Alasfour and Abdulrahim 2011). Using pinch technology and heat recovery to compensate for the temperature drop solve this problem. The highest exergy destruction belonged to the evaporator and then the compressor. The results showed that at the brine temperature of 70 °C and TBT of 90 °C, the exergy destruction in the evaporator was 2.5 times higher than that in the compressor. This value was reduced as the brine temperature of MVC was increased. An MEE-MVC plant (capacity of 1500 m^3/d) was investigated by Elsayed et al. (2019). The maximum second law efficiency of 2.8% was achieved in which the evaporator and MVC units were in charge of about 52% and 39% of the total exergy destruction, respectively (similar to the MSF-MVC process). The high values of exergy destruction in the evaporators confirmed that the evaporation was highly inefficient, requiring modification. It was concluded that thermal performance was enhanced while the number of desalination stages was 32 and 25 for MSF and MSF-TVC systems, respectively (Tayyeban et al. 2022). Increasing the number of effects from 1 to 6 reduced the SEC by 39% while increasing the second law efficiency by 70%. A photothermal system as a cost-effective, well-designed and high-efficiency evaporator solves this problem. It utilizes solar energy for energy conservation and desalination. This system can effectively and quickly generate steam when light absorbance enhances by special microstructures and materials (Lin et al 2022; Su et al. 2022). An MEE-TVC system (capacity of 2200 L/h) was designed by Kariman et al. (2019) in which the device was powered by electricity to evaporate wastewater. The results indicated that the central heat exchanger and boiler had high exergy destruction contributions. Working at the highest temperature led to the highest irreversibility in the heat exchanger. An MEE-TVC system was developed by Hyundai Heavy Industries (capacity of 4546–20,000 m^3/d) and its thermal performance was evaluated thermodynamically (Lee and Song 2005). A high exergy efficiency was achieved due to the lower energy consumption or the low-pressure motive stream needed for the TVC.

Different MEE-VC techniques (capacity of 4545 m^3/d) were thermionically evaluated by Sharaf et al. (2011). Two layouts of solar power cycles were considered to run the MEE-PF-VC plants. The minimum total solar field area of 14 m^2 led to the lowest overall exergy degradation rate, which was obtained at the minimum compression ratio. The effect of suction pressure on exergy destruction was investigated at a constant motive steam pressure in an MEE-VC plant (Zhou et al. 2019). Despite the low motive steam consumption, its exergy content increased at higher motive steam pressures, increasing the exergy destruction. In the investigated process, about half of the overall exergy destruction was related to the TVC and desuperheater, while 11% was attributed to the condenser and the first effect. The exergy destruction in TVC varied with the suction location

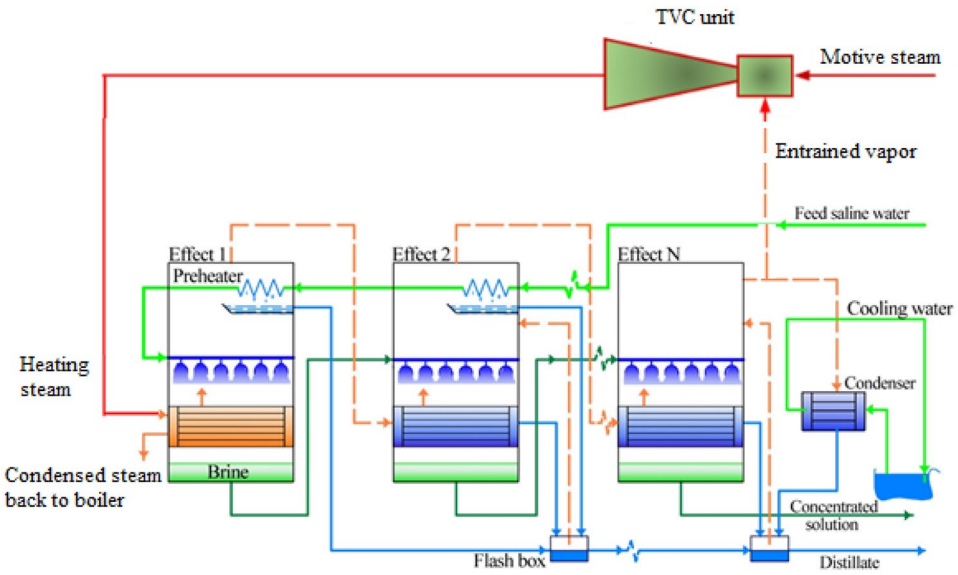

Fig. 7 Schematic of MEE-TVC desalination system

due to the differences between the quality of suction and motive steams. Using simulators for finding the best location can be proposed. ME-TVC, ME-TVC-MEE and ME-TVC with regenerative feed heaters (ME-TVC, FH) processes were exergetically analyzed by Alasfour et al. (2005). The steam ejector and evaporators were the main sources of irreversibility in all layouts. The reason was using high motive steam of the boiler at high temperature and pressure, increasing the discharge enthalpy into the first effect, causing a high destructive rate. High exergy destruction in the steam jet ejector was due to mixing, compression and expansion processes in the throat, nozzle and diffuser, respectively. The lowest exergy destruction was achieved in the second layout due to more heat recovery from the leaving stream using a regenerative feed heater, which reduced the irreversibility. For all layouts, increasing the motive steam pressure meaningfully increased the specific exergy destruction in the evaporators, ejector, condenser and leaving streams. A ME-TVC system was integrated into a gas turbine (GT) plant through heat recovery steam generator (HRSG) (Shakib et al. 2012). The main exergy-destructive components were the evaporator of HRSG, the steam jet ejector and economizer while the ME-TVC effects had the minimum exergy destruction.

A pressurized water reactor power plant was coupled to an MEE-TVC unit by Ansari et al. (2010). A schematic of the MEE-TVC process is shown in Fig. 7. The highest irreversibility occurred in the reactor followed by the steam generator, while the lowest value belonged to the moisture separator. The reactor had the maximum irreversibility owing to a very high destruction rate of the fission process and wasting about half of the fuel exergy. The performance of a ME-TVC system using an evaporative gas turbine (EvGT) was compared with a ME-TVC using a steam-injected gas turbine (STIG) by Wang and Lior (2007). Although the heat recovery in the HRSG by the motive steam/water at different pressures was similar, a higher pressure caused a more exergy-efficient heat transfer process. The enhanced exergy utilization in the HRSG was sufficient to compensate for the increased exergy consumption in the ME-TVC unit at high pressure. A system containing an ejector refrigeration cycle, MEE and gas combustion unit was developed by Saharkhiz et al. (2021). The wasted heat of the cycle provided the required heat to the desalination units. Using waste heat of each component for running a process or heating an appropriate stream should be considered in all hybrid desalination processes. The overall exergy efficiency of the system was estimated at 65.92%. The reactors (43.37%), heat exchangers (26.76%) and throttle valves (10.58%) had the highest contribution to exergy destruction in the combined system.

The exergy analysis of a solar–geothermal poly-generation plant was conducted using a dynamic simulation model by Calise et al. (2016). The system was equipped with an ORC fueled by a geothermal energy source and a parabolic trough collector. The results showed that the exergy efficiency varied between 40 and 50% during the thermal recovery mode and in the range of 16–20% during the cooling mode. The exergy analysis of the MEE plant coupled with the Rankine cycle (RC) showed that the highest exergy destruction belonged to the MEE and air-cooled condenser. Coupling the RC to the MEE system increased the turbine's exhaust stream exergy, increasing the exergy destruction in the MEE and air-cooled condenser after the turbine. The results indicated that the exergy contribution of the throttle valve increased at the plant part load operation, and the destructed exergy was higher whenever the ambient temperature was low (Mata-torres et al. 2019). Therefore, full-load operation and using a renewable energy driven air heater could be helpful.

An MEE combined with a reverse electrodialysis heat engine (MEE-RED) was studied exergetically by Hu et al. (2019). The RED, condenser and preheater units by accounting for ~ 60% of the overall exergy destruction were the main sources of irreversibility. The overall exergy efficiency of the system was 4.7%. Investigating a 6-effect MEE-membrane desalination plant (MEE-MD) with a capacity of 165,600 kg/d based on exergy destruction revealed the major extent of generated entropy (Farsi and Dincer 2019). The condenser of the MEE unit and the membrane module of the MD was the most exergy-destructive components. The high flow rate of the cooling water within the condenser with a low pipe wall thickness and small pore size (resulting in diffusional mass transfer resistance) of the membrane structure increased the irreversibility. An MEE-RO system (desalination capacity 10,304.3 m^3/d) using GT was designed by Mokhtari et al. (2016). Exergy was mostly destructed in the combustion chamber due to the entropy generation. HRSG and MEE were the next exergy-destructive components due to the high-temperature difference between the output and input flows. The thermodynamic study of a solar-assisted MEE-ORC-RO arrangement showed the most exergy-destructive component was the solar collector. An increase in the solar radiation intensity and collector length led to an increase in exergy destruction (Naminezhad and Mehregan 2022).

A heating, cooling, power and MEE system based on solid oxide fuel cell (SOFC)/GT was investigated through conventional and advanced exergy analyses. The exergy destruction was split into unavoidable/avoidable and exogenous/endogenous components to explore the real potential of exergy performance. The highest exergy destruction occurred in the burner, fuel cell and MEE system, accounting for 20.08%, 12.99% and 12.91%, respectively. The results indicated that the main exergy destructions were of endogenous type by the inverter, turbine and compressor. The exergy efficiency obtained via conventional

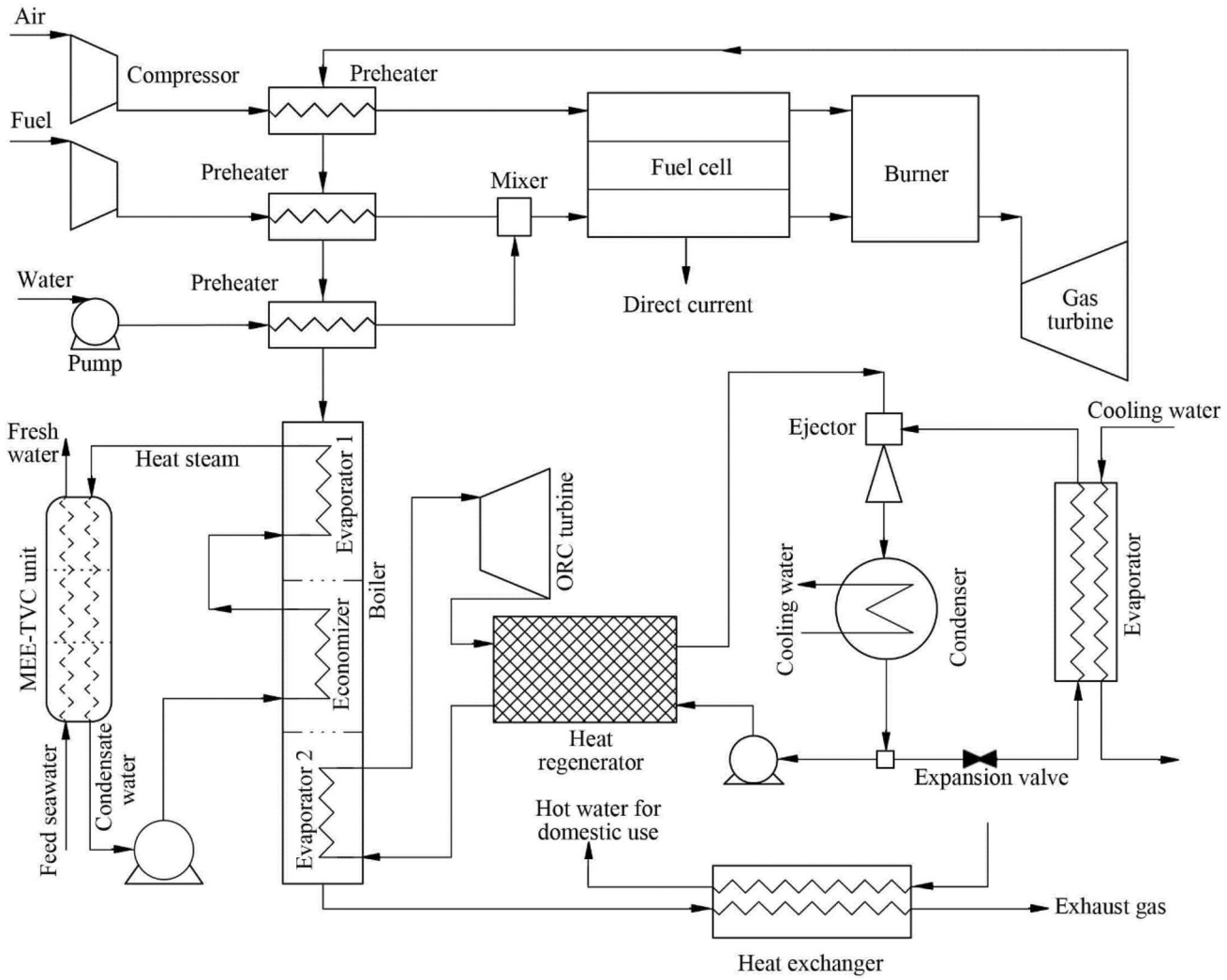

Fig. 8 Schematic of an MEE-TVC system integrated to fuel cell and gas turbine (You et al. 2020)

exergy investigation was lower than the advanced one due to a more detailed exergetic analysis of the process and components by advance approach. The first evaporator and MEE-TVC unit had the lowest potential for reducing the exergy destruction due to their low avoidable endogenous parts (You et al. 2020). A hybrid multi-generation system operated by a SOFC was proposed by Ghaebi and Ahmadi (2020). Figure 8 shows the schematic of an MEE-TVC desalination system integrated into the SOFC and GT. The system achieved an exergy efficiency of 63.04% where the fuel cell stack, afterburner, steam generator, compressor and pumps were recognized as the most to least exergy-destructive components. A higher exergy efficiency was attained by an increment in the inlet temperature of the fuel cell and compression ratio or by a decrease in the current density and pressure of the generator.

An HDH-HP system was proposed by Anand and Murugavelh (2020). The highest to lowest exergy destruction occurred in the evaporator, compressor, expansion device and condenser. Reducing the evaporator temperature and increasing the condenser temperature of the VC unit resulted in high exergy destruction due to the high-temperature difference between the environment and components. In the proposed system, the temperature difference between the evaporator and its hot humid air inlet was high, leading to its high exergy destruction. The compressor was the second largest exergy-destructive component, which was relatively lower than the air-cooled VC system. This was due to the reduced condensing temperature leading to a lower pressure ratio. Exergy analysis of a TVC-HDH-RO system (Fig. 9) was discussed by Al-Sulaiman et al. (2013). It was revealed that the highest exergy destruction occurred in the TVC

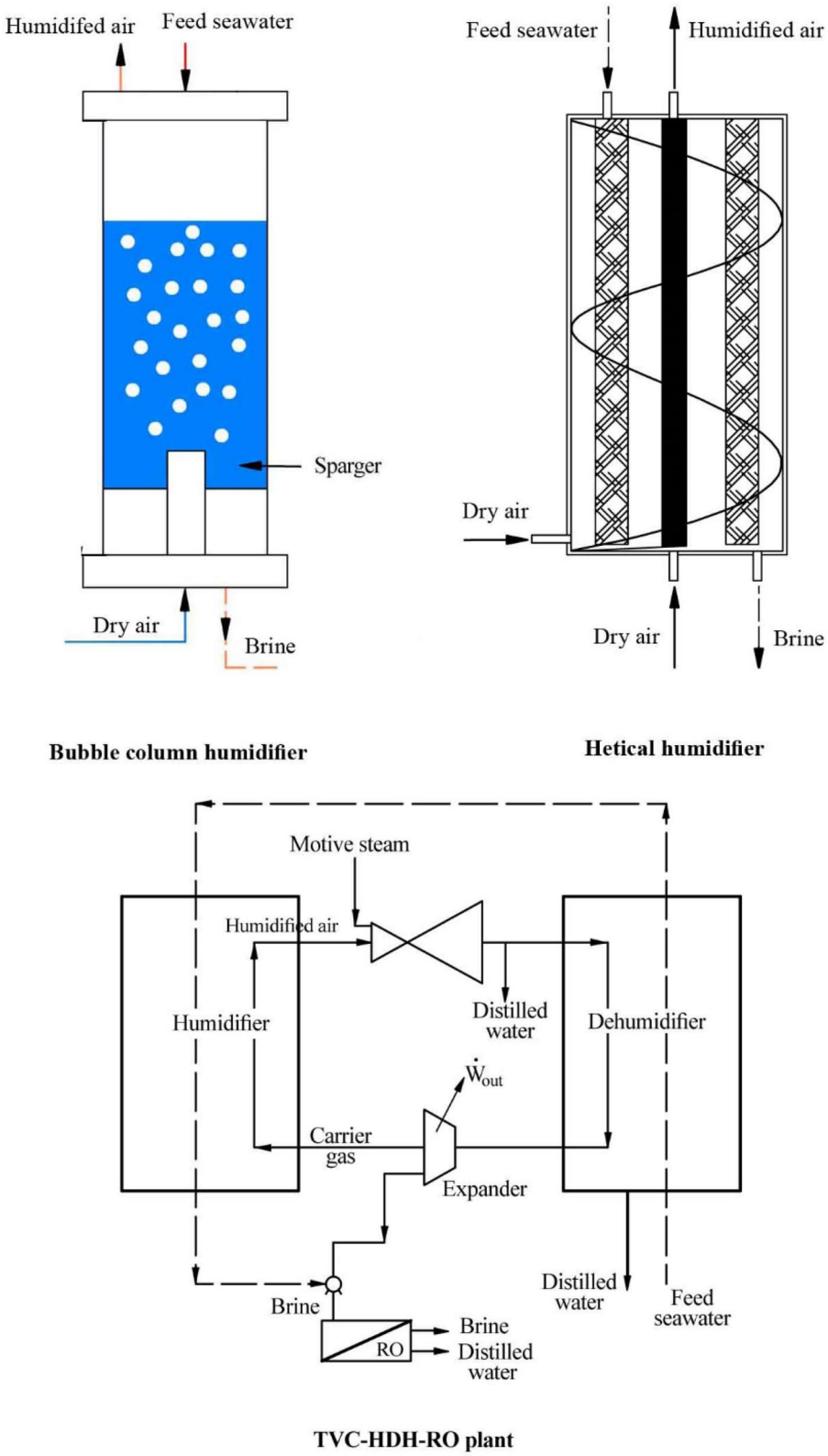

Fig. 9 Schematics of the bubble column and helical humidifiers, and TVC-HDH-RO system (Al-Sulaiman et al. 2013)

unit followed by the dehumidifier. The exergy efficiency of the system decreased as the steam pressure increased due to an increase in the energy flowing into the system. The total specific exergy destruction decreased by 130.7% as the expander efficiency increased from 40 to 90%.

Two layouts (i.e., series and parallel) of a geothermal-driven HDH-ORC system were investigated by Kolahi et al. (2020). Since the series layout produced higher output work, its exergy efficiency was greater than the parallel layout. In four cogeneration layouts of an ORC-HDH system investigated by Ariyanfar et al. (2016), the ORC with toluene had the highest energy and exergy efficiencies while the ORC with *n*-heptane as the working fluid had the highest cooling outlet temperature.

Thermodynamic analysis of three brine-recycled HDH systems with ZLD operation was investigated by Ghofrani and Moosavi (2020b). The compressor efficiency had a substantial influence on the irreversibility of the compressor and condenser. Reducing the compressor efficiency increased its irreversibility (owing to the higher power consumption) as well as the condenser exergy destruction (due to the higher power rejection to the ambient from the auxiliary condenser cooler). Later, they tried to decrease the water production cost of the conventional ZLD processes via an HDH-MEE-VC system (Ghofrani and Moosavi 2020a). To this end, 4 to 8 effects and 1 to 3 stages were considered for the MEE unit and the HDH system, respectively. More than half of the specific exergy destruction of the proposed system belonged to the thermo-compressors. Increasing the number of stages in the HDH system reduced the irreversibility; hence, the specific exergy destruction of all components of the HDH system decreased. Using bubble column humidifier due to its higher mass and heat transfer coefficients compared to other humidifiers (i.e., packed bed, spray tower, wet wall towers) can be proposed for HDH systems. The MEE condenser and the second thermo-compressor in the MEE-TVC/single-stage HDH plant had the minimum and maximum specific exergy destruction share, respectively. Figure 9 shows the schematic of the hybrid TVC-HDH-RO plant, and bubble column and helical humidifiers.

Performance comparison of the stand-alone and hybrid desalination processes

The performance indicators for several desalination plants are tabulated in Table 1. It is interpreted from this table that the MEE, HDH, MSF, VC and hybrid desalination systems can achieve an exergy efficiency that varies from 1.31% in an MSF-MEE system to 91.12% in a poly-generation system consisting of MEE, ammonia–water absorption and multi-refrigerant refrigeration systems. Notably, the exergetic efficiency should be used to compare the performance of similar components operating under similar conditions in the same or different systems. Different feed saline water and produced freshwater qualities, reference environments, inlet and outlet exergy fluxes, and equations for exergy efficiency calculation affect the overall exergy efficiency. These items cause one observe overall exergy efficiency in an extended range. For the comparison of dissimilar components, the only variable that should be used is the exergy destruction ratio. Hence, it is recommended to use the rates of exergy destruction to characterize the performance of system components considering the inefficiencies of the remaining system components. Furthermore, little attention has been given in some exergy analyses to the structure of the system and the mutual interdependencies among its components. Future studies using exergetic and exergoeconomic variables need to focus more on the mutual interdependencies among the components of a thermal system and on the calculation of the unavoidable exergy destruction for each component of a desalination system (Tsatsaronis 1999; Tsatsaronis and Cziesla 2004).

All stand-alone systems required modification or integration with other desalination plants due to their low exergy efficiency. The exergy efficiency of a desalination plant increased by coupling to a SOFC or HP, using surplus low-pressure steam or makeup steam and optimizing the effect and stage numbers. Designing a poly-generation system capable of producing power, desalinated water, liquefied natural gas (LNG), and heating and cooling effects could improve the system exergetically. The desalination systems benefit from an increased evaporation temperature using an RC cycle. HDH systems as a small-scale desalination system can be modified by coupling to a RO unit.

The best system can be selected among the described systems in terms of power consumption, freshwater production cost, GOR, freshwater productivity and exergy cost. The poly-generation system consisting of MEE, absorption and refrigeration systems with the capability of LNG production as well as MEE-TVC coupled with SOFC-GT can be good candidates to be further investigated.

Conclusion

The exergy analysis or entropy generation studies indicate the irreversibility of a process and its components which can optimize the system for efficient energy utilization. The minimization of exergy destruction and entropy generation is necessary to determine the operating conditions for optimum performance. A wide literature is available regarding different thermal desalination units individually

Table 1 Outputs of thermal desalination plants

Plant description		Process type	Max. energy consumption (kWh/m^3)	Min. water production cost ($/m^3)	Max GOR	Max. water production rate	Max. exergy efficiency (%)	Main observations	Ref
MEE		Stand-alone	0.097×10^{-3}	–	8	4500 m^3/d	5.3	The exergy destruction was decreased by modifying the material of the heat exchanger and system insulation 82% of the exergy was destructed by the MEE-TVC section, 48.6% of which was due to the TVC	Sadri et al. (2018)
MEE-AD (Adsorption)-RO		Hybrid system	00.053×10^{-3}	1.3	16	9300 m^3/d	19.92		
MEE-TVC integrated into solar RC (configuration C1)		Hybrid system	2.5	1.4	15	40,975 m^3/d	15	The freshwater costs of the MED and MED/TVC configurations were higher than that of the dual-purpose plants The freshwater cost was affected by the solar intensity rather than seawater temperature At a fuel price of 0.23 $/m^3 the freshwater cost of fuel-based dual-purpose plants was equal to that of the plants using solar energy	Askari et al. (2018)
MEE-TVC	FF	Hybrid system	144.3	2.3	5.78	5000 m^3/d	4.23	The maximum exergy destruction of 58% occurred in the TVC plant which was reduced by decreasing the pressure of the supplied motive steam The main cause of irreversibility was phase change, heat loss, pressure drop, and effluent and outlet streams	Elsayed et al. (2018b)
	BF		136.7	2.21	6.08		4.11		
	PF		137.4	2.16	6.05		4.03		
	PCF		131.8	2.09	6.31		4.31		
MEE-MVC		Hybrid system	8.29	1.64	6.7	5344 m^3/d	4.78	The MEE-VCHP process used less fuel exergy than the MEE-MVC owing to its higher seawater exergy content The first effect in the MEE-VCHP and MEE-MVC systems had the topmost exergy destruction rate. Nevertheless, in the MEE-ACHP, the absorber had the highest exergy destruction rate Using the brine waste heat decreased the exergy destruction of the MEE-MVC	Rostamzadeh et al. (2020)
MEE-ACHP (absorption–compression heat pump)			22.33	3.45	5.73	1962 m^3/d	3.81		
MEE-VCHP (vapor compression heat pump)			7.34	1.75	6.77	6020 m^3/d	5.3		

Table 1 (continued)

Plant description	Process type	Max. energy consumption (kWh/m^3)	Min. water production cost ($/m^3)	Max GOR	Max. water production rate	Max. exergy efficiency (%)	Main observations	Ref
MEE-MVC With makeup steam	Hybrid system	9.4	2.2	5.5	–	4.34	The heat exchangers had the minimum exergy efficiency Reducing the compressor outlet temperature decreased the exergy destruction of the desuperheater The exergy destruction in the first evaporator was reduced by heat recovery from exchangers and a decrease in the brine recirculation ratio Reducing the power consumption and temperature drop per evaporator as well as increasing the heating area of the evaporators led to higher exergy efficiency	Nafey et al. (2008)
MEE-MVC Without makeup steam			1.7	6		5.75		
MEE-MVC (4-effect)	Hybrid system	5.5	2	10.5	1500 m^3/d	7.5		
		4.7	2	12	5000 m^3/d			
MSF	Stand-alone	2.84	2.66	8	5000 m^3/d	–	The irreversibility decreased by increasing the module number due to reducing the temperature difference between the evaporators and the low temperature of the leaving streams	Nafey et al. (2006b)
MEE	Stand-alone	0.8	1.87	8				
MSF-MEE	Hybrid system	0.96	1.7	8.12		1.31		
HDH	Stand-alone	–	–	1.4		12.66	The exergy destruction in the HDH system was increased by raising the feedwater flow rate and its salinity The flat plate collector was responsible for 90% of exergy destruction Adding two parallel stand-alone HDH units reduced the exergy efficiency compared to the RO–HDH unit owing to the lower exergy efficiency of the stand-alone HDH unit	Ameri and Eshaghi (2016)
HDH-RO	Hybrid system			1.05	5.76 m^3/h	20.6		
HDH-RO	Hybrid system	3.8	0.11	14.5	–	2.88	An increase in the turbine and pressure exchanger efficiencies increased the total exergy efficiency due to the greater energy recovery and energy input The heater, humidifier and dehumidifier had maximum to minimum irreversibility The exergy efficiency could be enhanced using the throttling valves with an energy recovery component (e.g., pressure exchanger or Pelton turbine)	Jamil et al. (2018)
HDH-RO consisting of Pelton turbine		2.4		15.5		2.97		
HDH-RO consisting of pressure exchanger		2.05		16		3		

Table 1 (continued)

Plant description	Process type	Max. energy consumption (kWh/m^3)	Min. water production cost ($/m^3)	Max GOR	Max. water production rate	Max. exergy efficiency (%)	Main observations	Ref
MEE-TVC coupled with SOFC and GT	Cogeneration system	0.073	–	8.17	0.718 kg/s	66.32	Increasing the pressure ratio of the SOFC compressors enhanced the efficiency of the SOFC and GOR while decreasing the freshwater productivity Increasing the utilized steam in the SOFC and decreasing the utilization factor of the SOFC improved the second law efficiency due to the improvement in the generated power of the SOFC	Mohammadnia and Asadi (2020)
MEE-ORC	Cogeneration system	0.001	0.675	0.91	73 t/h	45	The most exergy-destructive equipment was the evaporator due to the large temperature difference between the outlet and inlet streams and the pressure drop The system performance was enhanced by utilizing a turbine or pump with high isentropic efficiency, using enriched propane in the hydrocarbon mixture of the working fluid, utilizing a highly energy-efficient heat exchanger, an eductor with a smaller diffuser angle and utilizing a high atomizing flash spray evaporator with swirl effect	Hosseini Araghi et al. (2016)
CCHP (combined cooling–heating–power)-MEE-TVC	Cogeneration system	–	–	8.87	85.57 kg/s	36.03	Owing to multiple products the CCHP cycle had higher exergy efficiency than the GT An increase in the turbine inlet temperature was equivalent to lower exergy destruction, although an opposite behavior was observed for exergy efficiency, due to the reduced mass flow rate and added heat to the cycle while the work output was constant The combustion chamber accounted for the majority of exergy destruction because of an increase in fuel consumption and a large temperature gap between the intake air and flame. The MEE-TVC unit was the second source of exergy destruction	Moghimi et al. (2018)
Solar RC-MEE	Stand-alone Cogeneration system	42.4 33.7	5.47 5.057	–	100 m^3/d	31.82 33.1	MEE-PF provided lower exergy destruction per solar collector against MEE-FF due to the lower feed flow rate	Sharaf et al. (2011)

Table 1 (continued)

Plant description	Process type	Max. energy consumption (kWh/m^3)	Min. water production cost ($/m^3)	Max GOR	Max. water production rate	Max. exergy efficiency (%)	Main observations	Ref
MEE-TVC-RO-ORC	Cogeneration system	7.71	3.08	8.71	–	26.2	The solar collectors, wind turbines, MEE, RO, evaporator, condenser, turbine and pump had the maximum to minimum share of exergy destruction The most exergy-destructive component in the ORC was the evaporator	Makkeh et al. (2020)
MEE (23-effect) coupled to an electrodialysis heat engine	Cogeneration system	35.4	–	–	–	23.8	The MEE unit was the main source of exergy destruction Using high-performance membranes and optimization of the inlet solutions concentration and velocity were recommended	Giacalone et al. (2019)
MEE-ACHP	Cogeneration system	–	–	9.88	15,000 m^3/d	22.95	The MEE, pump, expansion valve, absorber, heat exchanger and generator had the lowest to highest exergy efficiencies The exogenous exergy destruction was lower than endogenous exergy destruction. The avoidable exogenous and endogenous exergy destruction rates at the absorber assembly/expansion valve were higher than those at the generator	Janghorban Esfahani et al. (2015)
TVC-MEE combined cycle power plant (8 effects)	Cogeneration system	0.062×10^{-3}	–	9.47	–	7.6	Using 34% of the fuel input, the maximum useful work was generated by the GT engines; however, they were the major sources of irreversibility The minimum exergy destruction (3.3%) occurred in the steam turbine due to the reheating unit and type of the working fluid A minor increase in exergy efficiency resulted from integrating a preheater into the desalination unit The exergy efficiency of the ME-TVC-MEE plant was higher due to the higher utilization of waste exergy in effects and the increase in the useful work of separation	Almutairi et al. (2016)

Table 1 (continued)

Plant description	Process type	Max. energy consumption (kWh/m^3)	Min. water production cost ($/m^3$)	Max GOR	Max. water production rate	Max. exergy efficiency (%)	Main observations	Ref
MEE, absorption and refrigeration systems with capability of LNG production, 8-effect	Poly-generation system	0.23	1.5	13	1347 t/h	91.12	The highest amount of exergy destruction belonged to the heat exchangers By increasing the number of solar collectors, the energy efficiency was improved while the production cost was decreased	Ghorbani et al. (2019a)
MEE using a molten carbonate fuel cell	Poly-generation system	–	–	2.918	118,944 kg/h	88.95	• The fuel cell was the major source of exergy destruction • The generator had the highest exergy efficiency (98.7%)	Ghorbani et al. (2019b)
HDH-ACHP	Poly-generation system	–	–	1.7	367,092 kg/h	74.9	The most exergy-destructive component was the absorption refrigeration cycle; however, it caused a high overall exergy efficiency	Rostamzadeh et al. (2018)
CCPP-HDH	Poly-generation system	–	–	0.62	10 kg/h	17.12	Increasing the generator temperature, decreasing the refrigeration capacity and output power as well as the condenser temperature decreased the exergy efficiency For the 50% isobutane concentration, the output power and exergy efficiency reached their maximum values	Sadeghi et al. (2017)

or integrated with different systems. Such information is beneficial to identify the components which have room for modification of design and operational conditions to enhance the total exergy efficiency.

The following main conclusions have been drawn:

- In an MSF system, heat recovery and heat rejection stages, brine heater, leaving streams and pumps possessed the highest to lowest exergy destruction. Operating at a high TBT and flash stage number was recommended to improve the system performance.
- In an MEE process, the preheaters and heat exchanges were the main sources of irreversibility. Increasing temperature difference between the effects reduced the exergy destruction. The maximum second law efficiency was related to the P/CF followed by the FF, BF and PF configurations. Using waste heat and cascade heating was recommended.
- In the VC process, the evaporators and compressor shared the highest amount of exergy destruction. The distillate, pumps and brine preheater had the next rankings in terms of exergy destruction. Increasing the entrainment ratio of thermo-compressors and the number of effects, using a high-efficiency compressor with a low compression ratio and reducing the TBT and heating steam temperature increased the exergy efficiency in the VC process. Selecting a flash tank with a large volume in a VC flash desalination system, increasing the areas of the heaters and heat exchangers or using a high-efficiency heat exchanger, the exergetic performance of this process improved.
- In HDH systems, in a constant humidifier volume, the exergy efficiency could reach its highest value when a shorter humidifier with a larger diameter was designed. The lowest irreversible system loss occurred at an optimum value of the dry air mass flow rate. Increasing the dehumidifier-to-humidifier pressure ratio and decreasing the humidifier pressure in the variable pressure HDH system increased the exergy destruction. The highest exergy destruction occurred in the solar collector and rejected brine followed by the evaporator, compressor, expansion device and condenser.
- The MSF-MEE process could be modified to WGC-MSF-MEE-ORC to achieve higher exergy efficiency.
- In the MEE-TVC process, the major cause of exergy destruction was the TVC plant. In the reactor power plant coupled to an MEE-TVC, the highest irreversibility occurred in the reactor followed by the steam generator while the lowest value belonged to the moisture separator.
- In the GT-MEE-RO process, the highest to lowest exergy destruction occurred in the combustion chamber, HRSG and MEE units. In the TVC-MEE-CCPP system, the GT engines produced the greatest useful work while they were the major sources of irreversibility.
- In the MEE-MD process, the condenser of the MEE unit and the membrane module of MD was the most exergy-destructive elements. The high flow rate of the cooling water within the condenser as well as the thin thickness and the small pore size of the membrane structure led to high irreversibility.
- In the MEE-RED process, the RED, condenser and preheater were the main sources of irreversibility while in the MEE-TVC process using HRSG, the main sources of exergy destruction were the MEE plant, generator and ejector. In the ME-TVC-HRSG cycle, the main exergy-destructive components were the evaporator of the HRSG, the steam jet ejector and the economizer while in the ME-TVC system, the effects had the minimum exergy destruction.

Overall, it can be concluded that an idealized thermodynamic analysis of thermal desalination systems should be conducted. Exergy analysis confirmed that all stand-alone systems required modification or integration with other desalination plants due to their low exergy efficiency. The exergy efficiency of a desalination plant increased meaningfully by coupling to SOFC or ACHP, AD, RO, ABHP, using surplus low-pressure steam or makeup steam and optimizing the effect and stage numbers. Designing a polygeneration system capable of producing power, desalinated water and LNG as well as heating and cooling effects could improve the system exergetically. The desalination systems benefit from increasing the evaporation temperature using an RC cycle. Coupling the HDH process to an RO unit or TVC-RO plant, and using helical and bubble column humidifiers were also recommended to improve the system performance exergetically.

Acknowledgements The authors would like to thank Dr. M. Mastani for his cooperation in the language editing of the article.

Author contributions All sections has been written under the supervision of professor Hatamipour by Rahimi-Ahar.

Funding The authors would like to express their sincere gratitude to the Iranian National Science Foundation (INSF) [Grant number: 98011784, 2020] for financial support.

Data availability The authors confirm that the data supporting the findings of this study are available within the article.

Declarations

Conflict of interest The authors declare that they have no known competing financial interests or personal relationships that could have appeared to influence the work reported in this paper.

References

Abd Elrahman MA, Abdo S, Hussein E, Altohamy AA, Attia AAA (2020) Exergy and parametric analysis of freeze desalination with reversed vapor compression cycle. Therm Sci Eng Prog 19:100583. https://doi.org/10.1016/j.tsep.2020.100583

Abid A, Jamil MA, Sabah N, Farooq MU, Yaqoob H, Ali Khan L, Shahzad MW (2021) Exergoeconomic optimization of a forward feed multi-effect desalination system with and without energy recovery. Desalination 499:114808. https://doi.org/10.1016/j.desal.2020.114808

Al Ghamdi A, Mustafa I (2016) Exergy analysis of a MSF desalination plant in Yanbu, Saudi Arabia. Desalination 399:148–158. https://doi.org/10.1016/j.desal.2016.08.020

Alasfour FN, Abdulrahim HK (2011) The effect of stage temperature drop on MVC thermal performance. Desalination 265:213–221. https://doi.org/10.1016/j.desal.2010.07.054

Alasfour FN, Darwish MA, Bin Amer AO (2005) Thermal analysis of ME-TVC+MEE desalination systems. Desalination 174:39–61. https://doi.org/10.1016/j.desal.2004.08.039

Alhazmy MM (2014) Economic and thermal feasibility of multi-stage flash desalination plant with brine-feed mixing and cooling. Energy 76:1029–1035. https://doi.org/10.1016/j.energy.2014.09.022

Alkhulaifi YM, Baata E, Al-Sulaiman FA, Ibrahim NI, Ben-Mansour R (2021) Performance and exergoeconomic assessment of a novel combined ejector cooling with humidification-dehumidification (HDH) desalination system. Desalination 500:114843. https://doi.org/10.1016/j.desal.2020.114843

Almutairi A, Pilidis P, Al-mutawa N (2016) Energetic and exergetic analysis of cogeneration power combined cycle and ME-TVC-MED water desalination plant: part-1 operation and performance. Appl Therm Eng 103:77–91. https://doi.org/10.1016/j.applthermaleng.2016.02.121

Al-Sulaiman FA, Narayan GP, Lienhard JHV (2013) Exergy analysis of a high-temperature-steam-driven, varied-pressure, humidification–dehumidification system coupled with reverse osmosis. Appl Energy 103:552–561

Al-Sulatman DA, Ismail B (1995) Exergy analysis of major recirculating multi-stage flash desalting plants in Saudi Arabia. Desalination 103:265–270

Altmann T, Robert J, Bouma A, Swaminathan J, Lienhard VJH (2019) Primary energy and exergy of desalination technologies in a power-water cogeneration scheme. Appl Energy 252:113319. https://doi.org/10.1016/j.apenergy.2019.113319

Al-Weshahi MA, Anderson A, Tian G (2013) Exergy efficiency enhancement of MSF desalination by heat recovery from hot distillate water stages. Appl Therm Eng 53:226–233. https://doi.org/10.1016/j.applthermaleng.2012.02.013

Al-Weshahi MA, Tian G, Anderson A (2014) Performance enhancement of MSF desalination by recovering stage heat from distillate water using internal heat exchanger. Energy Procedia 61:381–384. https://doi.org/10.1016/j.egypro.2014.11.1130

Ameri M, Eshaghi MS (2016) A novel configuration of reverse osmosis, humidification – dehumidification and flat plate collector: modeling and exergy analysis. Appl Therm Eng 103:855–873. https://doi.org/10.1016/j.applthermaleng.2016.04.047

Anand B, Murugavelh S (2020) Performance analysis of a novel augmented desalination and cooling system using modified vapor compression refrigeration integrated with humidification-dehumidification desalination. J Clean Prod 255:120224. https://doi.org/10.1016/j.jclepro.2020.120224

Ansari K, Sayyaadi H, Amidpour M (2010) Thermoeconomic optimization of a hybrid pressurized water reactor (PWR) power plant coupled to a multi effect distillation desalination system with thermo-vapor compressor (MED-TVC) Reheat cooler Steam generator. Energy 35:1981–1996. https://doi.org/10.1016/j.energy.2010.01.013

Ariyanfar L, Yari M, Aghdam EA (2016) Proposal and performance assessment of novel combined ORC and HDD cogeneration systems. Appl Therm Eng 108:296–311. https://doi.org/10.1016/j.applthermaleng.2016.07.055

Ashrafizadeh SA, Amidpour M (2012) Exergy analysis of humidification-dehumidification desalination systems using driving forces concept. Desalination 285:108–116. https://doi.org/10.1016/j.desal.2011.09.041

Askari IB, Ameri M, Calise F (2018) Energy, exergy and exergoeconomic analysis of different water desalination technologies powered by linear fresnel solar field. Desalination 425:37–67. https://doi.org/10.1016/j.desal.2017.10.008

Aziz MA, Lin J, Mikšík F, Miyazaki T, Thu K (2022) The second law analysis of a humidification-dehumidification desalination system using M-cycle. Sustain Energ Technol Assess 52:102141. https://doi.org/10.1016/j.seta.2022.102141

Bandi CS, Uppaluri R, Kumar A (2016) Global optimization of MSF seawater desalination processes. Desalination 394:30–43. https://doi.org/10.1016/j.desal.2016.04.012

Calise F, Dentice M, Macaluso A, Piacentino A, Vanoli L (2016) Exergetic and exergoeconomic analysis of a novel hybrid solar–geothermal polygeneration system producing energy and water. Energy Convers Manag 115:200–220. https://doi.org/10.1016/j.enconman.2016.02.029

Carballo JA, Bonilla J, Roca L, De la Calle A, Palenzuela P, Alarcón-Padilla DC (2018) Optimal operating conditions analysis for a multi-effect distillation plant according to energetic and exergetic criteria. Desalination 435:70–76. https://doi.org/10.1016/j.desal.2017.12.013

Cerci Y (2002) The minimum work requirement for distillation processes. Energy Int J 2:15–23. https://doi.org/10.1016/S1164-0235(01)00036-X

Chen Q, KumJa M, Li Y, Chua KJ (2019) Energy, exergy and economic analysis of a hybrid spray-assisted low-temperature desalination/thermal vapor compression system. Energy 166:871–885. https://doi.org/10.1016/j.energy.2018.10.154

Chiranjeevi C, Srinivas T (2016) Exergy analysis of dehumidifier in a combined two stage desalination and cooling plant. J Chem Pharm Sci 3:86–90

Chung HW, Nayar KG, Swaminathan J, Chehayeb KM, Lienhard VJH (2017) Thermodynamic analysis of brine management methods: Zero-discharge desalination and salinity-gradient power production. Desalination 404:291–303. https://doi.org/10.1016/j.desal.2016.11.022

Deniz E, Çınar S (2016) Energy, exergy, economic and environmental (4E) analysis of a solar desalination system with humidification-dehumidification. Energy Convers Manag 126:12–19. https://doi.org/10.1016/j.enconman.2016.07.064

Dincer I, Cengel Y (2001) Energy, entropy and exergy concepts and their roles in thermal engineering. Entropy 3:116–149. https://doi.org/10.3390/e3030116

Dincer I, Rosen MA (2012) Exergy: energy, environment and sustainable development. Newnes. Second Edition. Elsevier.

Elhaj MA, Yassin JS (2013) Exergy analysis of a solar humidification-dehumidification desalination unit. Int J Mech Aerospace Ind Mechatron Manuf Eng 7:1697–1701

El-Nashar AM, Al-Baghdadi AA (1998) Exergy losses in a multiple-effect stack seawater desalination plant. Desalination 116:11–24. https://doi.org/10.1016/S0011-9164(98)00053-8

Elsayed ML, Mesalhy O, Mohammed RH, Chow LC (2018a) Transient performance of MED processes with different feed configurations. Desalination 438:37–53. https://doi.org/10.1016/j.desal.2018.03.016

Elsayed ML, Mesalhy O, Mohammed RH, Chow LC (2018b) Exergy and thermo-economic analysis for MED-TVC desalination systems. Desalination 447:29–42. https://doi.org/10.1016/j.desal.2018.06.008

Elsayed ML, Mesalhy O, Mohammed RH, Chow LC (2019) Transient and thermo-economic analysis of MED-MVC desalination system. Energy 167:283–296. https://doi.org/10.1016/j.energy.2018.10.145

Farahat MA, Fath HES, El-Sharkawy II, Ookawara Sh, Ahmed M (2021) Energy/exergy analysis of solar driven mechanical vapor compression desalination system with nano-filtration pretreatment. Desalination 509:115078. https://doi.org/10.1016/j.desal.2021.115078

Farsi A, Dincer I (2019) Development and evaluation of an integrated MED/membrane desalination system. Desalination 463:55–68. https://doi.org/10.1016/j.desal.2019.02.015

Feng Z, Zhou X, Xu S, Ding J, Cao S (2018) Impacts of humidification process on indoor thermal comfort and air quality using portable ultrasonic humidifier. Build Environ 133:62–72. https://doi.org/10.1016/j.buildenv.2018.02.011

Ghaebi H, Ahmadi S (2020) Energy and exergy evaluation of an innovative hybrid system coupled with HRSG and HDH desalination unit. J Clean Prod 252:119821. https://doi.org/10.1016/j.jclepro.2019.119821

Ghaffour N, Bundschuh J, Mahmoudi H, Goosen MFA (2015) Renewable energy-driven desalination technologies: a comprehensive review on challenges and potential applications of integrated systems. Desalination 356:94–114. https://doi.org/10.1016/j.desal.2014.10.024

Ghofrani I, Moosavi A (2020) Brine elimination by hybridization of a novel brine-recycle bubble-column humidification-dehumidification system with a multiple-effect distillation system. Energy Convers Manag 217:113004. https://doi.org/10.1016/j.enconman.2020.113004

Ghofrani I, Moosavi A (2020) Energy, exergy, exergoeconomics, and exergoenvironmental assessment of three brine recycle humidification-dehumidification desalination systems applicable for industrial wastewater treatment. Energy Convers Manag 205:112349. https://doi.org/10.1016/j.enconman.2019.112349

Ghorbani B, Shirmohammadi R, Amidpour M, Inzoli F, Rocco M (2019) Design and thermoeconomic analysis of a multi-effect desalination unit equipped with a cryogenic refrigeration system. Energy Convers Manag 202:112208. https://doi.org/10.1016/j.enconman.2019.112208

Ghorbani B, Mehrpooya M, Ali S (2019b) Hybrid molten carbonate fuel cell power plant and multiple-effect desalination system. J Clean Prod 220:1039–1051. https://doi.org/10.1016/j.jclepro.2019.02.215

Giacalone F, Catrini P, Cipollina A, Piacentino A, Tamburini A, Micale G (2019) Reverse electrodialysis heat engine with multi-effect distillation: exergy analysis and perspectives. Energ Convers Manag 194:140–159. https://doi.org/10.1016/j.enconman.2019.04.056

Gude VG (2018) A comprehensive framework for thermoeconomic analysis of desalination systems. Chem Eng 2:28. https://doi.org/10.3390/chemengineering2020028

Guo P, Li T, Wang Y, Li J (2021) Energy and exergy analysis of a spray-evaporation multi-effect distillation desalination system. Desalination 500:114890. https://doi.org/10.1016/j.desal.2020.114890

Hamed OA, Zamamiri AM, Aly SI, Lior N (1996) Thermal performance and exergy analysis of a thermal vapor compression desalination system. Energy Convers Manag 37:379–387. https://doi.org/10.1016/0196-8904(95)00194-8

Hamed OA, A-sofi MAK, Imam M, Mustafa GM, Mardouf KB, A-washmi H (2000) Thermal performance of multi-stage flash distillation plants in Saudi Arabia. Desalination 128:281–292. https://doi.org/10.1016/S0011-9164(00)00043-6

Han D, He WF, Yue C, Pu WH (2017) Study on desalination of zero-emission system based on mechanical vapor compression. Appl Energ 185:1490–1496. https://doi.org/10.1016/j.apenergy.2015.12.061

He WF, Xu LN, Han D, Gao L, Yue C, Pu WH (2016) Thermodynamic investigation of waste heat driven desalination unit based on humidification dehumidification (HDH) processes. Appl Therm Eng 100:315–324. https://doi.org/10.1016/j.applthermaleng.2016.02.047

Hosseini Araghi A, Khiadani M, Hooman K (2016) A novel vacuum discharge thermal energy combined desalination and power generation system utilizing R290/R600a. Energy 98:215–224. https://doi.org/10.1016/j.energy.2016.01.007

Hou S, Zeng D, Ye S, Zhang H (2007) Exergy analysis of the solar multi−effect humidification−dehumidification desalination process. Desalination 203:403–409. https://doi.org/10.1016/j.desal.2006.03.532

Hu J (2019) Exergy analysis for the multi-effect distillation-reverse electrodialysis heat engine. Desalination 467:158–169. https://doi.org/10.1016/j.desal.2019.06.007

Jamil MA, Zubair SM (2017) Design and analysis of a forward feed multi-effect mechanical vapor compression desalination system: an exergo-economic approach. Energy 140:1107–1120. https://doi.org/10.1016/j.energy.2017.08.053

Jamil MA, Elmutasim SM, Zubair SM (2018) Exergo-economic analysis of a hybrid humidification dehumidification reverse osmosis (HDH-RO) system operating under different retrofits. Energy Convers Manag 158:286–297. https://doi.org/10.1016/j.enconman.2017.11.025

Jamil MA, Shahzad MW, Zubair SM (2020) A comprehensive framework for thermoeconomic analysis of desalination systems. Energy convers manag 222:113188. https://doi.org/10.1016/j.enconman.2020.113188

Janghorban Esfahani I, Lee SC, Yoo CK (2015) Evaluation and optimization of a multi-effect evaporation-absorption heat pump desalination based conventional and advanced exergy and exergoeconomic analyses. Desalination 359:92–107. https://doi.org/10.1016/j.desal.2014.12.030

Jin CZ, Chou QL, Jiao DS, Shu PC (2014) Vapour compression flash seawater desalination system and its exergy analysis. Desalination 353:75–83. https://doi.org/10.1016/j.desal.2014.09.001

Kahraman N, Cengel YA (2005) Exergy analysis of a MSF distillation plant. Energy Convers Manag 46:2625–2636. https://doi.org/10.1016/j.enconman.2004.11.009

Kariman H, Hoseinzadeh S, Heyns PS (2019) Energetic and exergetic analysis of evaporation desalination system integrated with mechanical vapor recompression circulation. Case Stud Therm Eng 16:100548. https://doi.org/10.1016/j.csite.2019.100548

Kerme ED, Orfi J, Fung AS, Salilih EM, Ud-Din Khan S, Alshehri H, Ali E, Alrasheed M (2020) Energetic and exergetic performance analysis of a solar driven power, desalination and cooling poly-generation system. Energy 196:117150. https://doi.org/10.1016/j.energy.2020.117150

Khalilzadeh S, Nezhad AH (2018) Utilization of waste heat of a high-capacity wind turbine in multi effect distillation desalination: energy, exergy and thermoeconomic analysis. Desalination 439:119–137. https://doi.org/10.1016/j.desal.2018.04.010

Kolahi MR, Amidpour M, Yari M (2020) Multi-objective metaheuristic optimization of combined flash-binary geothermal and humidification dehumidification desalination systems.

Desalination 490:114456. https://doi.org/10.1016/j.desal.2020.114456
Kotas TJ (1995) The exergy method of thermal plant analysis, 2nd edn. Krieger Publishing Company, Florida
Lawal DU, Zubair SM, Antar MA (2018) Exergo-economic analysis of humidification-dehumidification (HDH) desalination systems driven by heat pump (HP). Desalination 443:11–25. https://doi.org/10.1016/j.desal.2018.05.011
Lee HCT, Song YKS (2005) Performance improvement of multiple-effect distiller with thermal vapor compression system by exergy analysis. Desalination 182:239–249. https://doi.org/10.1016/j.desal.2005.03.018
Li C, Goswami Y, Stefanakos E (2013) Solar assisted seawater desalination: a review. Renew Sustain Energy Rev 19:136–163. https://doi.org/10.1016/j.rser.2012.04.059
Lin Z, Wu T, Jia B, Shi J, Zhou B, Zhu C, Wang Y, Liang R, Mizuno M (2022) Nature-inspired poly (N-phenylglycine)/wood solar evaporation system for high-efficiency desalination and water purification. Colloids Surf A Physicochem Eng Asp 637:128272. https://doi.org/10.1016/j.colsurfa.2022.128272
Makkeh SA, Ahmadi A, Esmaeilion F (2020) Energy, exergy and exergoeconomic optimization of a cogeneration systemintegrated with parabolic trough collector-wind turbine with desalination. J Clean Prod 273:123122. https://doi.org/10.1016/j.jclepro.2020.123122
Mastani Joybari M, Hatamipour MS, Rahimi A, Modarres FG (2013) Exergy analysis and optimization of R600a as a replacement of R134a in a domestic refrigerator system. Int J Ref 36:1233–1242. https://doi.org/10.1016/j.ijrefrig.2013.02.012
Mata-torres C, Zurita A, Cardemil JM, Escobar RA (2019) Exergy cost and thermoeconomic analysis of a rankine cycle + multi-effect distillation plant considering time-varying conditions. Energy Convers Manag 192:114–132. https://doi.org/10.1016/j.enconman.2019.04.023
Messineo A, Marchese F (2008) Performance evaluation of hybrid RO / MEE systems powered by a WTE plant. Desalination 229:82–93. https://doi.org/10.1016/j.desal.2007.07.028
Moghimi M, Emadi M, Mirzazade Akbarpoor A, Mollaei M (2018) Energy and exergy investigation of a combined cooling, heating, power generation, and seawater desalination system. Appl Therm Eng 140:814–827. https://doi.org/10.1016/j.applthermaleng.2018.05.092
Mohammadnia A, Asadi A (2020) A hybrid solid oxide fuel cell-gas turbine fed by the motive steam of a multi-effects desalination-thermo vapor compressor system. Energy Convers Manag 216:112951. https://doi.org/10.1016/j.enconman.2020.112951
Mokhtari H, Sepahvand M, fasihfar A (2016) Thermoeconomic and exergy analysis in using hybrid systems (GT+MED+RO) for desalination of brackish water in persian gulf. Desalination 399:1–15. https://doi.org/10.1016/j.desal.2016.07.044
Mussati SF, Aguirre PA, Scenna NJ (2004) Improving the efficiency of the MSF once through (MSF-OT) and MSF-mixer (MSF-M) evaporators. Desalination 166:141–151. https://doi.org/10.1016/j.desal.2004.06.068
Muthusamy C, Srithar K (2017) Energy saving potential in humidification-dehumidification desalination system. Energy 118:729–741. https://doi.org/10.1016/j.energy.2016.10.098
Nafey AS, Fath HES, Mabrouk AA (2006a) Exergy and thermoeconomic evaluation of MSF process using a new visual package. Desalination 201:224–240. https://doi.org/10.1016/j.desal.2005.09.043
Nafey AS, Fath HES, Mabrouk AA (2006b) Thermo-economic investigation of multi effect evaporation (MEE) and hybrid multi effect evaporation-multi stage flash (MEE-MSF) systems. Desalination 201:241–254. https://doi.org/10.1016/j.desal.2005.09.044
Nafey AS, Fath HES, Mabrouk AA (2008) Thermoeconomic design of a multi-effect evaporation mechanical vapor compression (MEE-MVC) desalination process. Desalination 230:1–15. https://doi.org/10.1016/j.desal.2007.08.021
Naminezhad A, Mehregan M (2022) Energy and exergy analyses of a hybrid system integrating solar-driven organic rankine cycle, multi-effect distillation, and reverse osmosis desalination systems. Renew Energy 185:888–903. https://doi.org/10.1016/j.renene.2021.12.076
Nematollahi F, Rahimi A, Gheinani TT (2013) Experimental and theoretical energy and exergy analysis for a solar desalination system. Desalination 317:23–31. https://doi.org/10.1016/j.desal.2013.02.021
Omidi B, Rahbar N, Kargarsharifabad H, Rashidi S (2020) Combination of a solar collector and thermoelectric cooling modules in a humidification–dehumidification desalination system-experimental investigation with energy, exergy, exergoeconomic and environmental analysis. Energy Convers Manag 225:113440. https://doi.org/10.1016/j.enconman.2020.113440
Piacentino A, Cardona E (2010) Advanced energetics of a multiple-effects-evaporation (MEE) desalination plant. Part II: potential of the cost formation process and prospects for energy saving by process integration. Desalination 259:44–52. https://doi.org/10.1016/j.desal.2010.04.037
Rafat E, Babaelahi M (2020) Recovering waste heat of a solar hybrid power plant using a Kalina cycle and desalination unit: a sustainability (emergo-economic and emergo-environmenal) approach. Energy Convers Manag 224:113394. https://doi.org/10.1016/j.enconman.2020.113394
Rahimi B, Chua HT (2017) Low grade heat driven multi-effect distillation and desalination. John Fedor
Rahimi-Ahar Z, Hatamipour MS, Ghalavand Y (2018) Experimental investigation of a solar vacuum humidification-dehumidification (VHDH) desalination system. Desalination 437:73–80. https://doi.org/10.1016/j.desal.2018.03.002
Rahimi-Ahar Z, Hatamipour MS, Rahimi Ahar L (2020a) Air humidification-dehumidification process for desalination: a review. Prog Energy Combust Sci 80:100850. https://doi.org/10.1016/j.pecs.2020.100850
Rahimi-Ahar Z, Hatamipour MS, Ghalavand Y, Palizvan A (2020b) Comprehensive study on vacuum humidification-dehumidification (VHDH) desalination. Appl Therm Eng 169:114944. https://doi.org/10.1016/j.applthermaleng.2020.114944
Rahimi-ahar Z, Hatamipour MS (2020) A perspective of thermal type desalination: Technology, current development and thermodynamics analysis. Encyclopedia of Life Support Systems (EOLSS). http://www.eolss.net/Eolss-sampleAllChapter.aspx
Ranjan KR, Kaushik SC (2013) Energy, exergy and thermo-economic analysis of solar distillation systems: A review. Renew Sustain Energy Rev 27:709–723. https://doi.org/10.1016/j.rser.2013.07.025
Rostamzadeh H (2021) A new pre-concentration scheme for brine treatment of MED-MVC desalination plants towards low-liquid discharge (LLD) with multiple self-superheating. Energy 225:120224. https://doi.org/10.1016/j.energy.2021.120224
Rostamzadeh H, Ghavami S, Shekari A, Ghaebi H (2018) A novel multigeneration system driven by a hybrid biogas-geothermal heat source, part I: thermodynamic modeling. Energy Convers Manag 177:535–562. https://doi.org/10.1016/j.enconman.2018.08.088

Rostamzadeh H, Ghiasirad H, Amidpour M, Amidpour Y (2020) Performance enhancement of a conventional multi-effect desalination (MED) system by heat pump cycles. Desalination 477:114261. https://doi.org/10.1016/j.desal.2019.114261

Sadeghi M, Yari M, Mahmoudi SMS, Jafari M (2017) Thermodynamic analysis and optimization of a novel combined power and ejector refrigeration cycle–desalination system. Appl Energy 208:239–251. https://doi.org/10.1016/j.apenergy.2017.10.047

Sadri S, Khoshkhoo RH, Ameri M (2018) Optimum exergoeconomic modeling of novel hybrid desalination system (MEDAD+RO). Energy 149:74–83. https://doi.org/10.1016/j.energy.2018.02.006

Saharkhiz MHM, Ghorbani B, Ebrahimi A, Rooholamini S (2021) Exergy, economic and pinch analyses of a novel integrated structure for cryogenic energy storage and freshwater production using ejector refrigeration cycle, desalination unit, and natural gas combustion plant. J Energy Storage 44:103471. https://doi.org/10.1016/j.est.2021.103471

Salimi M, Akbarpour Reyhani H, Amidpour M (2018) Thermodynamic and economic optimization of multi-effect desalination unit integrated with utility steam network. Desalination 427:51–59. https://doi.org/10.1016/j.desal.2017.11.013

Sato N (2004) Chemical energy and exergy: an introduction to chemical thermodynamics for engineers. Elsevier

Senatore SJ (1979) Vapor compression distillation. Desalination 31:135–144. https://doi.org/10.1016/s0011-9164(00)88512-4

Shakib SE, Amidpour M, Aghanaja C (2012) Simulation and optimization of multi effect desalination coupled to a gas turbine plant with HRSG consideration. Desalination 285:366–376. https://doi.org/10.1016/j.desal.2011.10.028

Shakib SE, Amidpour M, Boghrati M, Ghafurian MM, Esmaieli A (2021) New approaches to low production cost and low emissions through hybrid MED-TVC+RO desalination system coupled to a gas turbine cycle. J Clean Prod 295:126402. https://doi.org/10.1016/j.jclepro.2021.126402

Sharaf MA, Soliman AM (2017) A novel study of using oil refinery plants waste gases for thermal desalination and electric power generation: energy, exergy and cost evaluations. Appl Energy 195:453–477. https://doi.org/10.1016/j.apenergy.2017.03.052

Sharaf MA, Nafey AS, García-Rodríguez L (2011) Thermo-economic analysis of solar thermal power cycles assisted MED-VC (multi effect distillation-vapor compression) desalination processes. Energy 36:2753–2764. https://doi.org/10.1016/j.energy.2011.02.015

Sharaf MA, Nafey AS, García-rodríguez L (2011) Exergy and thermo-economic analyses of a combined solar organic cycle with multi effect distillation (MED) desalination process. Desalination 272:135–147. https://doi.org/10.1016/j.desal.2011.01.006

Shariati M, Ghorbani B, Amidpour M, Hayati R (2019) Developing a hybrid integrated structure of natural gas conversion to liquid fuels, absorption refrigeration cycle and multi effect desalination (exergy and economic analysis). Energy 189:116162. https://doi.org/10.1016/j.energy.2019.116162

Sharqawy MH, Zubair SM (2011) On exergy calculations of seawater with applications in desalination systems. Int J Therm Sci 50:187–196. https://doi.org/10.1016/j.ijthermalsci.2010.09.013

Sharqawy MH, Antar MA, Zubair SM (2017) Performance evaluation of variable pressure humidification-dehumidification systems. Desalination 409:171–182. https://doi.org/10.1016/j.desal.2017.01.025

Shukuya M, Hammache A (2002) Introduction to the concept of exergy for a better understanding of low-temperature-heating and high-temperature-cooling systems. Publisher VTT Technical Research Centre, Finland

Spiegler KS, El-Sayed YM (2001) The energetics of desalination processes. Desalination 134:109–128. https://doi.org/10.1016/S0011-9164(01)00121-7

Su J, Zhang P, Yang R, Wang B, Zhao H, Wang W, Wang C (2022) MXene-based flexible and washable photothermal fabrics for efficiently continuous solar-driven evaporation and desalination of seawater. Renew Energy 195:407–415. https://doi.org/10.1016/j.renene.2022.06.038

Sundari KG, Ponnaganti V, Kumar TMN (2013) Exergy analysis of a low temperature thermal desalination system. Int J Mech Eng Rob Res 2:284–289

Szargut J, Morris DR, Steward FR (1988) Exergy analysis of thermal, chemical and metallurgical, Processes. Hemisphere Publication Corp, New York

Tang Y, Liu Z, Shi C, Li Y (2018) A novel steam ejector with pressure regulation to optimize the entrained flow passage for performance improvement in MED-TVC desalination system. Energy 158:305–316. https://doi.org/10.1016/j.energy.2018.06.028

Tayyeban E, Deymi-Dashtebayaz M, Dadpour D (2022) Multi objective optimization of MSF and MSF-TVC desalination systems with using the surplus low-pressure steam (an energy, exergy and economic analysis). Comp Chem Eng 160:107708. https://doi.org/10.1016/j.compchemeng.2022.107708

Tiwari GN, Sahota L (2018) Renewable Energy Powered Desalination Handbook Exergy and Technoeconomic Analysis of Solar Thermal Desalination. Elsevier Inc. https://doi.org/10.1016/B978-0-12-815244-7.00014-3

Tsatsaronis G (1999) Strengths and limitations of exergy analysis. Thermodynamic optimization of complex energy systems. Springer, Dordrecht, pp 93–100

Tsatsaronis G, Cziesla F (2004) Exergy, energy system analysis and optimization, strengths and limitations of exergy analysis. Encyclopedia of life support systems (EOLSS)

Vadalia BV, Patel P, Patel J (2014) Review on solar humidification-dehumidification process for pure water production. Int J Adv Res 2:951–961

Wang Y, Lior N (2007) Performance analysis of combined humidified gas turbine power generation and multi-effect thermal vapor compression desalination systems Part 2: The evaporative gas turbine based system and some discussions. Desalination 207:243–256. https://doi.org/10.1016/j.desal.2006.06.013

Woldai A (2016) Multi-stage flash desalination: modeling, simulation, and adaptive control. CRC Press Taylor and Francis Group, Singapore

Wu G, Kutlu C, Zheng H, Su Y, Cui D (2017) A study on the maximum gained output ratio of single-effect solar humidification-dehumidification desalination. Sol Energy 157:1–9. https://doi.org/10.1016/j.solener.2017.08.014

Yildirim C, Solmuş I (2014) A parametric study on a humidification-dehumidification (HDH) desalination unit powered by solar air and water heaters. Energy Convers Manag 86:568–575. https://doi.org/10.1016/j.enconman.2014.06.016

You H, Han J, Liu Y (2020) Conventional and advanced exergoeconomic assessments of a CCHP and MED system based on solid oxide fuel cell and micro gas turbine. Int J Hydrogen Energy 45:2143–12160. https://doi.org/10.1016/j.ijhydene.2020.02.138

Zheng H (2017) Solar energy desalination technology. Elsevier Inc, Amsterdam

Zhou S, Gong L, Liu X, Shen S (2019) Mathematical modeling and performance analysis for multi-effect evaporation/multi-effect evaporation with thermal vapor compression desalination system. Appl Therm Eng 159:113759. https://doi.org/10.1016/j.applthermaleng.2019.113759

Zhou S, Liu X, Bian Y, Shen S (2020) Energy, exergy and exergoeconomic analysis of a combined cooling, desalination and power system. Energy Convers Manag 218:113006. https://doi.org/10.1016/j.enconman.2020.113006